DEPARTMENT OF MECHANICAL ENGINEERING

UNIVERSITY OF UTAH
SALT LAKE CITY, UTAH 84112

D D C
RECEIVED
MAR 8 1972
D

R 93

CREEP FRACTURE IN ROCK IN UNIAXIAL
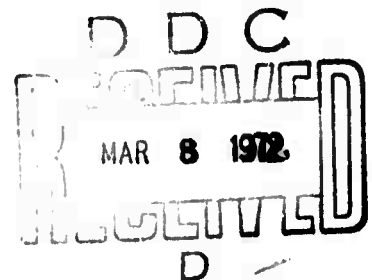# COMPRESSION

by

Wolfgang R. Wawersik
and
Wayne S. Brown

December 1971

Mechanical Engineering Department
College of Engineering
University of Utah
Salt Lake City, Utah 84112

DOCUMENT CONTROL DATA - R & D

(Security classification of title, body of abstract and indexing annotation must be entered when the overall report is classified)

1. ORIGINATING ACTIVITY *(Corporate author)*	2a. REPORT SECURITY CLASSIFICATION
University of Utah, Salt Lake City, Utah 84112	Unclassified
	2b. GROUP

3. REPORT TITLE

Creep Fracture in Rock in Uniaxial Compression

4. DESCRIPTIVE NOTES *(Type of report and inclusive dates)*

Final report (July 29, 1970 - October 31, 1971)

5. AUTHOR(S) *(First name, middle initial, last name)*

Wolfgang R. Wawersik and Wayne S. Brown

6. REPORT DATE	7a. TOTAL NO. OF PAGES	7b. NO. OF REFS
December 1971	85	57

8a. CONTRACT OR GRANT NO. H0110054	9a. ORIGINATOR'S REPORT NUMBER(S)
b. PROJECT NO. 1579	UTEC ME 71-242
c.	9b. OTHER REPORT NO(S) *(Any other numbers that may be assigned this report)*
d.	

10. DISTRIBUTION STATEMENT

Distribution of the document is unlimited.

11. SUPPLEMENTARY NOTES	12. SPONSORING MILITARY ACTIVITY
	Advanced Research Project Agency

13. ABSTRACT

Three rock types, a granite, a sandstone and a marble, were tested in uniaxial compression to assess the time dependent properties of brittle rocks at stress levels exceeding half the uniaxial compressive strength. Specimens were tested in quasi-static tests and in creep and differential creep experiments at room temperature. The effect of (partial) pore water pressure was considered by comparing air-dried and water-saturated samples. The influence of time and pore water pressure was qualitatively demonstrated in quasi-static experiments at strain rates between $0(10^{-5})$ to $0(10^{-3})$ sec^{-1}. Particular mathematical descriptions of time dependent deformations were derived from creep and differential creep tests. Some statistical data indicate that alternative constitutive equations may be developed. The strength of granite and sandstone varied considerably with time and pore water pressure. In general, a strong correlation was observed between the reduction of rock strength and the tendency of rock to creep on one hand and the characteristics of the complete quasi-static stress-strain curves on the other. It appears that time dependent deformation and failure are significant phenomena in so-called class II rocks. To predict time dependent failure of brittle rock a new approach was developed which combines the data of short-term creep tests with the results of controlled quasi-static experiments. The approach is deemed promising in the light of satisfactory agreement between predicted and measured creep fracture times.

DD FORM 1473
NOV 65

14. KEY WORDS	LINK A		LINK B		LINK C	
	ROLE	WT	ROLE	WT	ROLE	WT
Rock mechanics						
Complete quasi-static stress-strain curves						
Creep						
Time dependent rock failure						
Constitutive relations						

ARPA Order Number: 1579

Program Code Number: OFIO

Name of Contractor:
University of Utah

Effective Date of Contract:
July 29, 1970

Contract Expiration Date:
October 31, 1971

Amount of Contract $42,863.00

Contract Number: HO 110054

Principal Investigators and
Phone Number:
W. R. Wawersik, and W. S. Brown
801-581-6441

Project Scientist or Engineer
and Phone Number:
Same

Short Title of Work:
Creep Fracture in Rock
in Uniaxial Compression

FINAL REPORT

Sponsored by
Advanced Research Project Agency
ARPA Order No. 1579

December 1971

ACKNOWLEDGMENTS

TABLE OF CONTENTS

FIGURE CAPTIONS

SUMMARY

Three rock types, a granite, a sandstone and a marble were tested in uniaxial compression to assess the time dependent properties of brittle rocks at stress levels exceeding half the uniaxial compressive strength. Specimens were studied in quasi-static tests and in creep and differential creep experiments at room temperature ($76°F$). The effect of time on the behavior of brittle rocks was qualitatively demonstrated in quasi-static experiments in the range of strain rates from $O(10^{-5})$ sec^{-1} to $O(10^{-3})$ sec^{-1}. Mathematical descriptions of time dependent deformations were derived from creep and differential creep tests. The following relationships were developed between stress and the strain parallel to the applied compression.

Westerly granite:

$$\frac{d\epsilon}{dt} = 1.33 \times 10^{-20} \; \epsilon^{1-\frac{1}{n}} \; e^{11.44\frac{\sigma}{\sigma^*}} + 7.17 \times 10^{-20} \; e^{21.6\frac{\sigma}{\sigma^*}} \qquad (i)$$

Nugget sandstone:

$$\frac{d\epsilon}{dt} = 2.11 \times 10^{-25} \; \epsilon^{1-\frac{1}{n}} \; e^{19.83\frac{\sigma}{\sigma^*}} + 1.339 \times 10^{-20} \; e^{27.2\frac{\sigma}{\sigma^*}} \qquad (ii)$$

Tennessee marble:

$$\epsilon_I = 10^C \log t \qquad (iii)$$

n and σ^* are experimentally determined constants. C denotes an undetermined function of stress.

Time dependent deformation in granite and sandstone is strongly enhanced by a change of the pore water pressure from 0.1 pis to 12.3 psi. The results suggest that the effect of pore water pressure on the time

dependent deformation can be modeled by a differential equation of the form

$$\frac{d\varepsilon}{dt} = \bar{B}e^{\frac{\bar{N}-G(P)}{n}\frac{\sigma}{\sigma*}}e^{\frac{\bar{N}G(P)}{na}}\varepsilon^{1-\frac{1}{n}} + \bar{A}e^{n(1 + H(P))\frac{\sigma}{\sigma*}} \qquad (iv)$$

$G(P)$ and $H(P)$ are functions of the pore water pressure, P. Although Equations (i), (ii), and (iv) only describe the relationship between stress and the most compressive principal strain in uniaxial compression they are more general than most existing "creep laws." In principle they are valid under both constant and time varying stress conditions. Cursory statistical data analyses indicate that alternative descriptions of the time dependent behavior of rock may be developed. As more data are obtained, therefore, other constitutive equations might be proposed which are mathematically simpler and more suitable for use in design calculations.

Time dependent rock failure is of little importance in Tennessee marble but may pose hazards in Westerly granite and Nugget sandstone. The long term strengths of granite and sandstone are considerably lower than their quasi-static compressive strengths which are commonly measured on air-dried samples at a strain rate of approximatley 10^{-5} sec^{-1}.

To predict the time dependent strength of brittle rock a new and convenient approach was developed which combines the data of short-term creep experiments with the results of controlled quasi-static-tests. Satisfactory agreement was obtained between the predicted and measured failure times at different stress levels.

In general, a strong correlation was observed between the reduction of rock strength and the tendency of rock to undergo appreciable time

dependent deformations on one hand and the characteristics of the complete quasi-static stress strain curves on the other. It appears that time dependent deformation and failure are significant phenomena in class II rocks, i.e. rocks which exhibit an "unstable" failure behavior once their peak load bearing ability has been reached.

INTRODUCTION

Knowledge about the time-dependent mechanical properties of rock subjected to constant stress has long been considered vital for the interpretation of numerous geological phenomena. More recently time-dependent rock properties have also been studied extensively to predict rock deformation and rock strength under dynamic loading conditions. Surprisingly, however, to date little consideration has been given to the possible consequences of time-dependent rock behavior in the large class of engineering problems which deal with the construction and long-term stability of structures in and on rock. It is difficult to understand this neglect of an area which in 1971 was given primary importance by a special commission of the International Society for Rock Mechanics. Most likely the time-dependent properties of rock have not been included in engineering design for three reasons:

1. Time-dependent rock deformations measured under constant stress conditions in the laboratory are seemingly small, i.e. negligible by comparison with the instantaneous or elastic rock response.

2. It is difficult to distinguish time-dependent rock deformations in situ from ground motions which are due to "external" changes, i.e. changes which are unrelated to the material properties. As a result it is difficult to recognize the importance of time dependent effects.

3. Presently available descriptions of time-dependent rock properties are fragmentary and too inadequate to be used in

design calculations. In addition, field monitoring
programs and laboratory experimentation which are
needed to furnish such descriptions are complex,
time consuming and costly.

While the long-term stability of many unlined underground openings
suggests that time-dependent rock behavior has no practical consequences,
there are also an impressive number of examples where time-dependent
effects are or may be appreciable. In several instances, tunnelling
contractors and mine operators have observed that rock surrounding
underground openings "squeezes" and exhibits signs of extensive time-
dependent fracturing. Both phenomena were reported to occur in a Utah
mine during an extended shut-down period. After three months several
mine drifts had closed to half or less of the original cross-sectional
area during a time when the mine geometry and, therefore, the stress
field induced by mining had remained unchanged. In some cases time-
dependent rock deformation can be arrested by rapid installation of
artificial supports; in others time-dependent changes continue even in
the presence of supports. Because supports have to counteract the time-
dependent effects, support loads are increased until the support resist-
ance is exceeded, rock flow occurs, and extensive rehabilitation work
becomes necessary.

The research which is described here represents a first systematic
attempt to assess the importance of time-dependent rock behavior in the
design of structures in rock and rock masses. Specifically, the study
was designed to:

1. determine under what condition time-dependent rock
   deformation may be significant;

2. develop procedures to determine constitutive relations
   which define strain as a function of stress state, time,
   and other important variables;

3. evaluate the conditions and predictability of time-
   dependent rock failure;

4. attempt to assess time-dependent changes in the rock
   fabric and whether such changes can be used to predict
   impending time-dependent rock failure in situ.

To achieve these objectives, three rock types, a granite, a
sandstone, and a marble, were tested in uniaxial compression. Specimens
were studied in quasi-static tests and in creep and differential creep
experiments.

A review of past work concerning the time-dependent mechanical
properties of rock is given first. It is followed by a discussion of
some pertinent points concerning the development of time dependent con-
stitutive equations and failure theories for rock. Then the experimental
details are presented and, finally, all experimental results are described,
analyzed, and their practical implications evaluated.

LITERATURE REVIEW

Most of all published data on time-dependent rock properties
pertains to and is restricted to rock behavior under conditions of
constant stress, temperature, and pore water pressure and before rock
failure takes place. Hence, most of the available information on time-

dependent rock properties neither suffices to describe the response of rock where stress, temperature, and pore water pressure are not fixed nor can it be used to predict how rock strength may change with time. In spite of these limitations, important clues may be derived from the large body of existing data particularly when it is compared and combined with similar but more extensive observations on metals and other materials.

When rock is subjected to constant stress which is suddenly applied at time zero, its response may be divided into four broad regions (1 - 16). First, an instantaneous strain is observed which consists of an elastic, i.e. recoverable, and an inelastic or permanent strain component. In addition, strain develops with time. The rock is said to creep until, at sufficiently high stress, temperature, or pore water pressure, failure occurs. Rock creep, which is the time-dependent strain of rock subjected to constant stress, follows a characteristic sequence of events which are commonly denoted primary, secondary, and tertiary creep or sometimes transient, steady-state, and accelerated creep. During primary creep strain develops rapidly but at a decelerating rate. During secondary creep rock deforms at a constant rate until during tertiary creep the strain rate increases and creep eventually terminates in failure. Whether or not all three creep stages are observed depends primarily on the magnitude of the applied stress, the temperature, and the pore water pressure. For example, tertiary creep appears to be non-existent at low stresses (compared with the quasi-static rock strength) and low temperatures and pore water pressures. In turn, all three creep states can generally be observed at high stress close to the "quasi-static" compressive strength.

A set of typical creep curves of a limestone subjected to triaxial compression ($\sigma_1 > \sigma_2 = \sigma_3$) is shown in Figure 1. The strain in Figure 1 denotes the strain parallel to the applied compression which is parallel to the axis of the rock cylinders commonly used in this type of experiments. A few measurements, where both the axial and the lateral strain have been monitored in uniaxial compression, suggests that the lateral strains exhibit the same basic features of creep described above (8,13).

In general, time-dependent strain of rock can also be divided into recoverable and permanent components. The recoverable strain is observed when the load acting on the specimen is removed or reduced. Most measurements indicate that the recoverable strain component decreases with increasing stress and temperature.

Known creep data on rock leaves no doubt that the time-dependent behavior of rock is strongly effected by temperature (9,13,17). A rise in temperature at a given constant stress results in increased creep rates in all creep stages. A relationship between time-dependent rock properties and water and pore water pressure is strongly suggested by several quasi-static uniaxial compression experiments where rocks of different moisture contents, i.e. different partial pore water pressures, were compared (18,19,20). For example, the strength of basalt under high vacuum (low partial water pressure) increased by fifty per cent over its air-dried strength measured in fixed strain rate experiments. Similarly, the strength of quartzitic shale and quartzitic sandstone decreased markedly as the moisture content of the rocks was raised

from eight percent to 100 percent. The effect of pore water pressure on the time-dependent rock behavior was recently evaluated quantitatively in crack propagation and failure studies on quartz and fused quartz in creep and differential creep experiments (21,22). These as well as other tests suggest that the effect of water initiates a pressure-sensitive corrosion reaction at the tips of pre-existing cracks or cracks that have formed during the initial loading process. Experiments on glass (23,24,25) suggest that this corrosion process is particularly strong in silicas. This is not to say, however, that water and pore water pressure besides changing the stress state in rock may not alter the time-dependent behavior of, say, carbonaceous materials. On the contrary, changes of rock strength and strain-to-failure in strain rate controlled tests under pore pressure (26,27) have shown that water and pore water pressure also influence the time-dependent behavior of limestone although the rate-controlling mechanisms probably are different.

Very few experiments have been conducted to determine the effect of hydrostatic confinement on the time-dependent properties of rock (2,3,7,12,28). Creep tests were conducted on Solenhofen limeston at differential stresses up 80,000 psi between 15,000 and 60,000 and at 150,000 psi confining pressure. In addition, constant strain rate tests were described for marble, Solenhofen limestone as well as for sandstone and a gabbro at strain rates ranging from 10^{-8} sec^{-1} to 10^2 sec^{-1} in the broad temperature range from 25^0C to 800^0C. Overall the amount of data that was generated in these tests is too small to arrive

at any meaningful conclusions. The majority of results appears to indicate, however, that creep and thus time effects in general are at least as pronounced in confining pressure tests as they are in uniaxial compression experiments if the stress difference between the greatest and least compression (differential stress $\sigma_1 - \sigma_3$) exceeds one half the ultimate strength. The exact behavior of rock in any particular case undoubtedly is influenced by the governing deformation and failure mechanisms which are known to change with confining pressure even in very brittle rocks such as granite.

Essentially no data exists on the time-dependent behavior of rock subjected to tension. Several beam bending and torsion experiments (4,5,29), however, suggest that the phenomenon is similar in nature and no less prevalent than in compression.

Numerous attempts have been made to describe the time dependent behavior of rock quantitatively. To achieve this end, all experimental data have been analyzed in one of the following three ways:

1. It is assumed that the time-dependent behavior of rock is linear* and can therefore be represented by linear viscoelastic models consisting of linear elastic (spring) and viscous (dashpot) elements.

2. Time dependent behavior is interpreted in terms of "laws which describe the observed phenomena of creep (for example) in terms of previously established quantities and laws of physics" (40). Physical theories of creep have been proposed on different levels:

_____

*Linearity implies that the requirements of additivity (superposition) and scalar multiplication are satisfied.

on the atomic, microscopic and macroscopic scale using the concept of thermal activation energy that predicts a temperature dependence of the form $\varepsilon \propto e^{-\Delta H/RT}$. The activation energy ΔH is an experimentally determined quantity. For example, the activation energy has been interpreted as the energy required to initiate self diffusion or as the activation energy of a corrosion reaction.

3. An empirical approach is chosen where curves are fitted to experimentally determined data. Although curve fitting may be considered scientifically unsatisfactory in presenting a description of the mechanism, it is nevertheless the prevailing technique used to develop constitutive relation and the one that imposes the least number of restrictions on actual material behavior at a time when the number of mechanisms governing time-dependent effects are poorly understood.

A small number of representative samples of the many time-dependent constitutive equations which have been proposed during the past two decades are listed here:

$$\varepsilon = A_0 + A_1 \log t + A_2 t \tag{1}$$

$$\varepsilon = A_0 + A_3 (1 - e^{-k_1 t}) + A_2 t \tag{2}$$

or

$$\varepsilon = \frac{A_3}{k_1} e^{-k_1 t} \tag{3}$$

$$\varepsilon = A_0 + A_1 \log t + A_4 e^{-k_2 t} + A_5 e^{-k_3 t} + A_6 e^{-k_4 t} + A_2 t \tag{4}$$

$$\varepsilon = A_0 + A_1 \log t + A_7 t^{k_5} + A_8 t^{k_6} + A_2 t \tag{5}$$

$$\dot{\varepsilon} = A_2 e^{-Q/RT} \sinh \left(\frac{\sigma}{\sigma_0}\right) \tag{6}$$

k_1 through k_6 are experimentally determined constants.

A_0 in equations (1) through (5) denotes the instantaneous rock response which is associated with any stress increment. A_2 is the rate of strain per unit of time during secondary creep. The remaining terms in equations (1) to (4) define primary creep under different loading conditions. It is interesting to note that equation (4) defines the "axial" time dependent strain in uniaxial compression. The "lateral" strain which was monitored simultaneously (8) was described by the equation

$$\varepsilon' = A_0' + A_1' \cdot \log t + A_2' t \tag{7}$$

If A_0 and A_0' are taken to define both instantaneous recoverable elastic and irreversible responses, then all coefficients in the above equations are functions of stress. Depending on which literature source is considered

$$A_i \propto \sigma$$

or
$$A_i \propto \sigma^n$$
$$e^{\sigma}$$
$$\sigma e^{\sigma}$$
$$\sinh \left(\frac{\sigma}{\sigma_0}\right)$$

Similarly, if temperature and pore water pressure are denoted T and P then

$$A_i \propto T$$

$$\text{or} \quad A_i \propto e^T$$

$$e^{-1/T}$$

$$p^n$$

Time dependent rock behavior was earlier characterized to comprise two discrete phenomena: time-dependent deformation without failure and time-dependent fracture or loss of load bearing ability. The onset of time dependent rock failure always coincides with the beginning of tertiary creep. In general, very little is known about time dependent rock failure. In geological problems the possibility that time-dependent fracture might occur is considered very remote. The phenomenon has only recently received attention by geologists and geophysicists who are concerned about creep on faults and earthquake prediction. In engineering, on the other hand, time-dependent failure which includes the effect of strain rate on rock strength has been studied extensively under dynamic loading conditions (e.g.30). However, because the times involved and the strain rates used are very small, the data which was obtained in such experiments can hardly be extrapolated to the life time of a semi-permanent underground structure. While the amount of available information is inadequate to fully assess the possibility or predict the occurrence of time-dependent rock failure in general, it is sufficient to suggest that the phenomenon poses a hazard under some conditions. Beside field observations in "squeezing" ground, there are numerous laboratory studies where rock strength was observed to decrease up to factors of

2 and 5 in brittle and ductile rocks respectively with variations in temperature, moisture content and strain rate in the range from 10^{-5} sec^{-1} to 10^{-8} sec^{-1}. (17-20,23)

The prevailing approach used in the interpretation of time-dependent rock failure data is derived from static fatigue analysis which were conducted on metals and glasses. (24,30-32) Accordingly, rock strength is measured in creep experiments and plotted versus time or the logarithm of time and extrapolated to infinite time. (3,6,33) Typically, the strength drops rapidly with an increase of loading time and approaches an asymptotic value. This asymptotic value was suggested to coincide with the stress level, σ_d, which defines the typical inversion point, i.e., the beginning of dilatancy in all quasi-static stress-volumetric strain curves (33). This argument is appealing because the stress σ_d marks the onset of micro-cracking in numerous studies (3,33-39). However, the argument neglects the fact that the onset of dilatancy is temperature dependent and possibly also a function of pore water pressure. A strength-time curve derived under any one set of conditions can therefore not be considered unique. Care should also be exercised in the generalization of the concept of micro-cracking because it is not known whether it is the only mechanism which might lead to a loss of rock strength. For example, at high confining pressure and temperature, rock creep is also associated with twin and translation gliding and with recrystallization which might influence the time dependent strength of rock. Most important, strength-failure time curves have only been measured in two instances in uniaxial compression experiments. If the

stress where dilatancy begins indeed defines the permanent rock strength,
then the loss of strength with time may be greatly pronounced under
confined conditions because of the smaller ratio σ_d/σ_c where σ_c is the
quasi-static compressive strength (generally determined at $0(10^{-5})$ sec.$^{-1}$).

An alternative approach to the prediction of time dependent rock
fracture was made in the proposal underlying this study. Here it was
suggested that the time dependent strength of rock could be predicted by
combining the results of creep and quasi-static compression experiments.
This new approach will be discussed in more detail in subsequent sections
of this report.

CONCEPTS AND SUGGESTIONS CONCERNING THE DESCRIPTION OF TIME-DEPENDENT ROCK DEFORMATION AND FAILURE

The preceeding literature review stresses the phenomenon of creep because it is best suited to provide a basic understanding of time dependent rock behavior and because most of the available information on time-dependent rock properties was determined in creep experiments. It must now be emphasized, however, that creep tests under conditions of constant stress, temperature, and pore water pressure alone are not and cannot be the only source for a complete description of time-dependent effects under time varying conditions. To generate a general theory of time-dependent rock behavior, differential creep experiments must be carried out where stress, time, temperature and pore water pressure are applied in discrete increments to determine the effects of changes in particular variables. This important fact has not been considered by a large number of investigators, probably because both stress state and environmental parameters can be considered constant in many geological problems. This latter assumption is clearly not valid in the majority of engineering applications. Here more general constitutive discriptions are needed.

A brief inspection of Equations 1 through 7 brings out an obvious dilemma. First of all, the different forms of the proposed constitutive equations suggest that time-dependent rock behavior is an extremely complex phenomenon because of the various mineralogical and textural features of different rock types and therefore, presumably because of the variety of possible rate controlling mechanisms. Practically, all of the equations are non-linear. In all cases the descriptions of time-dependent behavior requires

separate considerations of primary and secondary creep which, contrary to metal behavior, are of the same order of magnitude. In addition, comparison of equations (4) and (7) suggests that laws derived from measurements of one strain only, say parallel to the direction of loading in uniaxial compression, are not necessarily identical to the lateral strain-time or volumetric strain-time history even in initially homogeneous and isotropic rocks. More important, perhaps is the fact that the complexity of most of the proposed models poses difficulties in recognizing their generalized form where all three principal stresses are non-zero. There is no obvious way by which an exponential stress dependency or a stress dependency of the form $\sinh\left(\frac{\sigma}{\sigma_o}\right)$ can be applied to describe time-dependent rock deformation under confined conditions, in tension or torsion. Finally, most of the proposed constitutive equations were derived under very restricted conditions and cannot be assumed a priori to describe time-dependent effects where stress, temperature and pore water pressure are not constant. For example, there is a fundamental difference between the models of equations (2) and (3), i.e., between a total and an incremental strain theory. This can be shown as follows: For the sake of simplicity let

$$\epsilon = F_1 (\sigma, T) \, F_2 (t) = F_1 (\sigma, T) \, t \tag{8}$$

Equation (8) is analogous to equation (2 etc.) an alternative form of equation (8) would be

$$\frac{d\epsilon}{dt} = \dot{\epsilon} = F_1 (\sigma, T) \qquad \text{or} \qquad \epsilon = \int F_1 (\sigma, T) \, dt \tag{9}$$

Clearly, if at time zero a rock specimen were subjected to a constant

stress σ_1, then the strain at time t_1 would be

$$\varepsilon_1 = F_1 (\sigma, T) t_1$$

according to both equations (8) and (9). However, if the test were repeated and if at time t_1 the stress were suddenly changed by $\Delta\sigma$ from σ_1 to σ_2, then equation (8) would predict a change $\Delta\varepsilon$ due to the stress change $\Delta\sigma$

$$\Delta\varepsilon \approx 0$$

neglecting the instantaneous rock response for the moment. But according to equation (9)

$$\Delta\varepsilon = \Delta F_1 (\sigma, T) t_1$$

Which of the two formulations, equation (8) or (9) best describes actual rock behavior can only be determined by further experiments.

The restrictiveness of all of the listed constitutive equations can be further demonstrated by the following argument. If two identical rock samples A and B were subjected to constant stress σ_1 and σ_2 respectively, then equations (1) through (7) predict the two creep curves shown in Figure 2. Now suppose that at time t_1 the stress acting on specimen A were suddenly changed to σ_2. Because time is contained explicitly in all equations, i.e.,

$$\varepsilon = F_1 (\sigma, T) F_2(t) = G_1 (\sigma, T, t) \tag{10}$$

or

$$\dot{\varepsilon} = G_2 (\sigma, T, t) \tag{11}$$

equations (1) to (7) would predict that the creep curve for $t > t_1$ would be identical to the curve segment a-b shifted downward. At all

times the predicted strain rate is determined by the prevailing values of stress and time. Actual data of this kind, however, indicates that the creep curve for $t > t_1$ is similar to the curve segment c-a shifted to the right. This implies that the actual creep rate is more realistically defined by the current values of stress and strain. A formulation of this kind may be obtained simply by eliminating time in equation (11) using equation (10) such that

$$\dot{\epsilon} = G_3 \, (\sigma, \, T, \, \epsilon) \tag{12}$$

A constitutive description which employs the strain hardening model of equation (12) has been applied successfully to metals (30,31) and has been proposed recently for a marble and a sandstone (16).

It is well known that the time-dependent properties of rock as determined in creep, relaxation or constant strain rate experiments are surprisingly similar to the properties of metals (40-42), glasses, plastics, (43), rubber, asphalt and other materials (44). This similarity in behavior does not indicate that the governing mechanisms are the same in all of these materials. However, it does show that they all undergo a similar sequence of rate controlling, thermally activated changes (42). It is therefore not only phenomenologically but also physically justified to apply techniques which were previously developed for the description, for example, of solid propellants or asphalt. No attempt will be made here to review viscoelastic theories which are summarized and discussed in several extensive publications (44-49). Instead, only a few points shall be raised to amplify the

need to cross disciplinary lines more frequently than has been done in the past.

Time-dependent rock behavior involves non-linear theories which pose severe difficulties in actual problem solutions. However, as some results in the literature suggest, it may be that a linear description of rock properties introduces only small and tolerable errors. To estimate the errors that might arise in the description of non-linear behavior by means of linear models, methods can be employed which have been developed and discussed in the solid propellant literature (44). If such simplifications appear impermissible, other guides may be sought. For example, the form of the strain hardening model equation (12) indicates that time-dependent rock behavior might fall in the category of normal fading memory constitutive theory (44,49) and, therefore, might be modeled by an assemblage of non-linear springs and dashpots. Obviously the use of such a model would greatly facilitate the generalization of uniaxial creep and relaxation data. Finally, the current formulation of time-dependent material properties is cumbersome. Because all known results appear to suggest a form

$$\epsilon = F_1 (\sigma, T, P) F_2 (t) \tag{13}$$

there is no reason why time-temperature (43,44) and time-pore water pressure superposition principles cannot be used and equation (13) be expressed in the form

$$\epsilon = F_1' (\sigma, T_0, P_0) F_2' (\zeta)$$

where ζ denotes the so-called "reduced time". T_0 and P_0 are reference

values of temperature and pore water pressure. The possibility of applying time-temperature and time-pore water pressure superposition is strongly suggested by recent experimental results on granite (50) and fused quartz (22).

Time-dependent rock failure may well be as important as the development of time-dependent deformations. To evaluate the potential danger of time-dependent rock failure the classical prediction scheme (32,46) is both time consuming and costly because failure times must be determined directly as a function of stress and environmental conditions. A new and easier approach was pursued in this study using the creep properties and the complete quasi-static stress-strain curves of rock. The approach is based on the hypothesis that time dependent failure occurs when rock has been strained a critical amount. Moreover, it is assumed that the greatest allowable strain prior to failure under constant environmental conditions is only a function of the stress state and independent of the loading history. This means that the time dependent failure of rock can be predicted by comparing the time dependent deformations with the allowable strain. The time dependent strains can be calculated from suitable constitutive equations. The allowable strain in turn is provided by complete quasi-static stress-strain curves. The method is advantageous in that it allows the possibility of time dependent failure to be assessed by means of routine quasi-static experiments and by means of creep tests of relatively short duration. The approach of using creep and quasi-static stress-strain data to predict time dependent rock failure was first suggested from results of a series of pilot creep and relaxation experiments which are shown in Figure 3.

Although the test conditions were very restrictive, the concept is deemed reasonable in principle. Strain has been used previously as a measure for impending rock failure (51). Strain criteria have also proven valid for some elastomers subjected to tension (52).

ROCK TYPES AND SPECIMENS

Westerly granite, Nugget sandstone and Tennessee marble were chosen for this study. All three rock types have been tested extensively (53,54,39) in the past, and therefore, have well defined properties. Some pertinent properties are listed in Table 1.

Rock	Grain Size (mm)	Porosity (%)	Major Constituents
Westerly granite	0.75	0.9	microline, quartz and anonthosite in approximately equal parts
Nugget sandstone	larger mode 0.135 smaller mode 0.07	7	quartz
Tennessee marble	2.3	0.37	calcite

Table 1. Rock Properties

The three rock types exhibit different types of failure behavior. Tennessee marble is known for its stable or class I (38) post-failure behavior which is associated with a gradual loss of load bearing ability in uniaxial compression. Westerly granite and Nugget sandstone

or both characterized by an unstable or class II (38,39) failure behavior. Failure in these rocks is inherently violent and leads to an instantaneous loss of strength in uniaxial compression once the peak stress has been reached.

Cylindrical sample one inch in diameter by approximately 2.3 inches in length were used. All specimens of each rock type were drilled in one direction out of the same block. For Nugget sandstone, specifically, the bedding planes lay perpendicular to the sample axes. All specimen surfaces were ground prior to testing. The specimen ends were machined parallel to within 0.0002 inches.

Both air-dried and water-saturated samples were tested. Air-dryness was achieved by exposing each specimen to room conditions at relatively constant humidity ratio, (0.0045 to 0.005) and temperature (76°F). The humidity ratio was determined by measuring the wet- and dry-bulp temperatures. Water saturated samples were obtained in the following manner. Each sample was first evacuated in a vacuum chamber for one and one-half hours at 5×10^{-2} Torr (6.6×10^{-2} mb). Tap water was then injected into the chamber so as to submerge the specimen, and a 50 psi pressure was applied to insure that the water would penetrate the specimen interior. All water-saturated samples were subsequently stored in water-filled containers. During testing the water-saturated samples were contained in loosely fitting water-filled jackets which were sealed at the top and bottom loading platens of the testing machine.

LOADING APPARATUS AND INSTRUMENTATION

Three loading apparatus were built for this study. All loading systems have identical design and are capable of generating both tensile and compressive forces. Each loading frame consists of a precision, double acting hydraulic cylinder, four tie rods, and crossheads designed to sustain 120 kip (Figure 4). Two of the hydraulic rams have capacities of 50 kip; the third one has a capacity of 89 kip at 3,000 psi pressure. If necessary, the capacities of the cylinders can be increased by sixty per cent simply by changing the capacity of all pressure lines to 5,000 psi. Accurage alignment of the loading frames is assured by carefully machined spacer tubes which fix the relative positions of the upper and lower machine cross-heads. A schematic of the three loading systems is shown in Figure 6.

The displacement of and the force generated by the loading pistons of the three hydraulic rams is controlled by regulating the hydraulic pressure in each cylinder. The hydraulic pressure in turn is generated optionally by means of a Sprague air pump or by means of a high-pressure gas accumulator. To limit the piston travel during tests which remain unattended over long time spans, solenoid valves are placed between the pressure source and each hydraulic cylinder. These solenoid valves are actuated and release the cylinder pressure when the piston travel has reached a predetermined amount.

All loading apparatus were used for both quasi-static and for creep experiments. To maintain a constant force a high pressure gas accumulator was pressurized in series with each hydraulic cylinder for subsequent load control (Figure 6). As soon as the desired load (stress) value was

reached, the pressure source was isolated from the loading systems and the load was then held constant to within plus forty pounds by means of the gas accumulator.

Force was measured either by means of load cells or with a 2,500 psi pressure gage. Each load cell is instrumented with four 500 Ω bounded foil strain gages which are connected externally into a four-arm Wheaston bridge circuit. The load cells were used exclusively to measure force in all quasi-static experiments. The pressure gage was employed to monitor the force in every long-term test.

Strain measurements were limited to the measurement of axial sample strain parallel to the direction of loading. The axial strain was determined indirectly by measuring end-to-end sample displacements. This method was chosen primarily because it eliminates errors due to micro-cracking if strain gages are bonded directly onto the rock surfaces. Indirect measurement of strain is imperative in water-saturated rock because both strain gages and bonding agents deteriorate rapidly under these conditions. End-to-end sample displacements were initially obtained by means of strain gage instrumented beryllium copper cantilever beams mounted at opposite sides of the sample diameter. Because of secondary creep problems in these transducers, the cantilevers were subsequently replaced by pairs of DCDT transducers as shown in Figure 4. Average displacement readings were ascertained by adding the outputs of each pair of transducers in a summing circuit. A schematic of the summing circuits which were specially built for this purpose is depicted in Figure 7. The accuracy of strain measurement with the latter system depends primarily on the quality of the line voltage regulation, the long-term stability of the transducers, DC power supplies, the summing amplifiers, and of the

recording equipment. Careful long-term calibration tests have shown that strains can be resolved to within 5×10^{-6} in short term creep tests (not exceeding five hours) and to within $\pm 20 \times 10^{-6}$ in long term experiments provided the test temperature (room temperature) does not vary by more than $1^{o}F$ as is usual in this laboratory.

EXPERIMENTAL PROCEDURE AND DATA ACQUISITION

All tests were conducted under uniaxial compression. Each specimen was loaded between two cylindrical steel spacers which had the same diameter as the rock samples. Quasi-static experiments were carried out at strain rates between 10^{-5} sec^{-1} and up to approximately 5×10^{-4} sec^{-1}. Complete stress-strain curves were obtained using an incremental loading technique which was developed earlier and which is described in detail in the literature (38). In all creep tests the rock was deformed at a strain rate of approximately $10^{-5}sec^{-1}$ until the predetermined stress value was reached From then on, the load was maintained constant. The relatively slow low strain rate during load application was selected deliberately to be able to compare the creep strain up to fracture (creep fracture) with results which were previously determined in quasi-static compression experiments.

Creep strains in rock are small in comparison with the "instantaeous" rock response between zero stress and the stress level at which creep is observed. Therefore, to determine creep strain accurately, high resolution in all strain measurements is imperative. To obtain this high resolution while operating in a given range of the strip-chart recorder or of the digital data acquisition system in general, only five per cent of the strain during loading up the desired constant stress was monitored. This means that most of the strain during load appccation was suppressed

by applying a bucking voltage to the summing circuits, i.e. by continuous zero balancing of the DCDT outputs (Figure 7). For subsequent analysis, the "instantaneous" or initial strain between zero stress and the creep stress level was assumed to be identical to the average response of each rock type which was observed in earlier quasi-static tests.

Differential creep tests were conducted in an analogous manner. After creep had proceeded at one stress level, the stress was suddenly raised to a second stress level and then held constant while the strain was monitored versus time.

Force-displacement data in quasi-static experiments were monitored continuously on an x-y recorder. All force displacement curves were subsequently converted into uniaxial stress-strain diagrams after subtraction of that portion of the displacement which was due to the deformation of the loading platens within the active gage length (Figure 4). Stress and strain were calculated using the original sample dimensions. Appreciable errors result after the specimen strength has dropped to 55% or 60% of its maximum value. Strain data from short-term creep experiments were plotted continuously versus time on a strip-chart recorder, or alternatively, strain readings were recorded with the digital data acquisition system (Figure 5), which was triggered manually at desired time intervals. In long-term experiments, strain was monitored continuously in the primary creep stage. Once secondary creep had begun, all strain readings were taken intermittently at intervals between two minutes and sixty minutes by means of the digital data acquisition system.

To identify the details of failure in both quasi-static compression and in creep, several samples were deformed to points along the descending branch of the complete stress-strain curve and also to points along the creep curve up to impending fracture. Once the desired fracture state was reached, the specimens were unloaded, cast in expoxy, sectioned and polished. The polished sections were then viewed under the microscope.

EXPERIMENTAL RESULTS

Approximately 45 quasi-static and 150 creep and creep fracture experiments were conducted on Westerly granite, Nugget sandstone and Tennessee marble. The experimental program was divided into three phases. During phase I, the quasi-static properties of aid-dried and water saturated rock samples wes determined at strain rates of approximately $10^{-5}sec^{-1}$ to $10^{-3}sec^{-1}$. During phase II, the time dependent behavior of all rocks were evaluated in creep and differential creep experiments as a function of stress and pore water pressure. The stress was varied in the range $0.5\sigma c \leq \sigma \leq \sigma'$, where σ_c denotes the quasi-static compressive strength of air-dried samples at $10^{-5} sec^{-1}$. The pore water pressure was varied indirectly by comparing air-dried and water saturated samples, i.e. by changing the partial pore water pressure between from 0.1 psi to 12.3 psi. Phase III served to assess a possible and measureable relationship between time dependent rock deformation and damage of the rock fabric which develops with time.

Quasi-Static Rock Properties

Figures 8 to 10 show three sets of complete, quasi-static stress-strain curves which are representative of all the results. Typical

individual rather than "average" stress-strain curves are given and several curves have been entered where the observed behavior between tests exhibited considerable variations. The mean compressive strength for each rock is listed in the figures. A comparison of the stress-strain curves of air-dried and water-saturated samples indicates that the presence of water strongly effects the mechanical behavior of Westerly granite and Nugget sandstone while it has virtually no influence on the stress-strain characteristics of Tennessee marble. All three rocks are clearly effected by the strain rate. An increase of the strain rate does not only result in an increase of the rock strength but also raises the strain where failure occurs: all three rocks become "tougher". Both the ascending and descending branches of the complete stress-strain curves are altered. However, it is interesting to note that the general shape of the complete stress-strain curves and the nature of the failure behavior, class I or class II, i.e. "stable" or "unstable" behavior, remain unchanged.

Time Dependent Deformations

Some difficulty arises in the presentation of the creep data which are most suitable for the derivation of time-dependent constitutive relations. For the sake of clarity, all data are given exclusively in graphical form. Typical creep curves for water-saturated Westerly granity, Nugget sandstone, and Tennessee marble are depicted in Figures 11 through 15. The duration of these creep experiments which were carried out on granite and sandstone.

Even a cursory inspection of Figures 11 through 16 brings out three important points.

1. The creep behavior of the three rocks appears to exhibit the well known stages of primary, secondary and tertiary creep.

2. Creep terminates in creep fracture even at relatively low stress levels. For example, the strength of water-saturated Nugget sandstone dropped to 19,000 psi after 1,200 hours compared with the quasi-static compressive strength of 33,400 psi in the air-dried state.

3. Both granite and sandstone exhibit a strain-hardening rather than time-hardening behavior under varying stress. In fact, the instantaneous strain rate which is associated with an almost instantaneous change of stress is even greater than would be predicted by the simple strain hardening model which was discussed earlier (Equation 12).

To develope a mathematical description of creep, a detailed analysis of all creep data was conducted. Cross plots of what appeared to be primary and secondary creep curves showed that the strains in Westerly granite and Nugget sandstone are proportional to t^n during primary creep and to t during secondary creep where t denotes time. Specifically it was found that

$$\epsilon_I = 10^C t^n \tag{15}$$

$$\dot{\epsilon}_{II} = 10^{C'} \tag{16}$$

ϵ_I and ϵ_{II} denote the strains during primary and secondary creep, respectively. C and C' are functions of stress. Published results on creep of a variety of materials suggested that the creep strains might

be related to a power function or to an exponential function of stress. Because the specific relationship between creep and stress was masked by considerable experimental scatter, simple regression analyses were carried out to correlate the quantities C and C' with the stress σ as well as the logarithm of stress. Also, correlation factors were obtained to evaluate the possible dependency of the exponent n in equation 15 and the stress. The results of this effort are given in Table 2.

n	C	C'	σ	log σ	Correlation factor, R
			Westerly granite		
x			x		0.108
	x		x		0.6942
	x			x	0.6885
		x	x		0.858
	x			x	0.825

n	C	C'	σ	log σ	Correlation factor, R.
			Nugget sandstone		
x			x		0.323
	x		x		0.413
	x			x	0.426
		x	x		0.627
	x			x	0.64

Table 2. Statistical Data Correlation

By and large the correlation factors are high enough to justify a fit of the observed creep data to any one of the suggested models. In particular it appeared permissible to assume that the creep strains of Westerly granite and Nugget sandstone are proportional to e^σ, i.e. $10^C \propto 10^{C'} \propto e^\sigma$. The exponent n in Equation 15 was taken to be independent of stress.

To determine the stress dependency of creep exactly, Figures 16 to 19 were prepared. The values of n in Figures 16 and 18 denote the slopes of all curves of $\log \epsilon_I$ versus $\log t$. The variable C is the primary creep strain which is reached one hour after load application. The linear fit of the data in Figures 17 and 19 defines the relationship between the rate of secondary creep, $\dot{\epsilon}_{II}$, and stress.

Figures 17 through 19 obviously exhibit a great deal of scatter which required many tests to be run in order to establish trends with reasonable realiability. No adequate explanation can be offered for this scatter. Because of precise specimen machining and because of the reproducibility of numerous long-term calibration tests, it is deemed highly unlikely that the results were effected by inadequate extraneous experimental conditions.

As shown in detail in appendix, the data reduction rendered the following description of the time dependent strain which assumes the validity of the strain hardening model of Equation 12:

Westerly granite
$$\frac{d\epsilon}{dt} = \dot{\epsilon} = 1.33 \times 10^{-20} \epsilon^{1-\frac{1}{n}} e^{11.44\frac{\sigma}{\sigma*}} + 7.17 \times 10^{-20} e^{21.6\frac{\sigma}{\sigma*}} \quad (17)$$

$$n = 0.392$$

$$\sigma* = 18,750 \text{ psi}$$

Nugget sandstone

$$\dot{\varepsilon} = 2.11 \times 10^{-25} \, \varepsilon^{1-\frac{1}{n}} \, e^{19.83\frac{\sigma}{\sigma*}} + 1.339 \times 10^{-20} \, e^{27.2\frac{\sigma}{\sigma*}} \quad (18)$$

$$n = 0.29$$

$$\sigma* = 16{,}700 \text{ psi}$$

The differential Equations 17 and 18 relate the strain increments to the stress $\sigma = \sigma(t)$. If the stress is held constant, then Equations 17 and 18 yield:

Westerly granite

$$\varepsilon = 8.7 \times 10^{-8} \, e^{4.49\frac{\sigma}{\sigma*}} \, t^{0.392} + 7.17 \times 10^{-20} e^{21.6\frac{\sigma}{\sigma*}} \, t \quad (19)$$

Nugget sandstone

$$\varepsilon = 10^{-7} \, e^{5.75\frac{\sigma}{\sigma*}} \, t^{0.29} + 1.339 \times 10^{-20} \, e^{27.2\frac{\sigma}{\sigma*}} \, t \quad (20)$$

In the stress range, $\sigma* \leq \sigma < 27{,}000$, the creep strain in Westerly granite can also be represented by Equation 21:

$$\varepsilon = 5.02 \times 10^{-5} \times t^{0.392} + 1.339 \times 10^{-20} \, e^{27.2\frac{\sigma}{\sigma*}} \, t \quad (21)$$

Here primary creep is assumed to be stress independent.

Neither equations 17, 18, 21 and Equations 19 and 20 include the effect of temperature and pore water pressure. In the light of published data (12, 13, 17), there is not doubt that an increase of temperature enhances creep. Exactly how the dependent strain of granite and sandstone is related to temperature goes beyond the scope of this pilot study. Using the results of Figures 16 through 19, some clues may be derived concerning the influence of pore water pressure. Clearly,

lowering the partial pore water pressure from 12.3 psi to 0.1 psi is associated with substantial reductions of the creep rates during primary and secondary creep. For example, the decrease of the secondary creep rate $\dot{\varepsilon}_{II}$ sec.$^{-1}$ in Westerly granite amounts to almost two orders of magnitude regardless of the level of the applied uniaxial compressive stress. In general, it appears from Figures 16 through 19 that the creep data for different partial pore water pressures render lines which are either displaced parallel to or rotated and displaced parallel to the straight lines which describe the creep of water saturated samples. Parallel displacements without rotation imply that the time dependent strains of granite and sandstone might obey an equation of the form:

$$\dot{\varepsilon} = \bar{B} \, e^{\frac{\bar{N}-G(P)\sigma}{n}}{\sigma^*} \, e^{\frac{\bar{N}G(P)}{na}} \, \varepsilon^{\frac{1-1}{n}} + \bar{A}e^{n(1 + H(P))\frac{\sigma}{\sigma^*}} \qquad (22)$$

where G(P) and H(P) are unknown functions of the pore water pressure P which govern the creep during the primary and secondary creep stages, respectively. It is noteworthy that Equation 22 is in qualitative agreement with data which was recently published for fused quartz. It is also noteworthy that Equation 22 probably can be simplified by introducing a "reduced" stress or a "reduced" time which would eliminate the pore pressure P. Obviously, the influence of pore pressure ought to receive further attention because of the strong effects which were observed in this study.

In constrast to granite and sandstone, creep in Tennessee marble was subordinate and resolvable only in the very narrow stress range $0.85\sigma_c \leq \sigma \leq \sigma_c$. In addition, the effect of partial pore water pressure

was negligible. In general, the creep of marble appeared to lack the secondary creep stage even where time dependent deformations terminated in creep functure. Primary creep was approximated by an expression of the Form:

$$\varepsilon_I = 10^C \log t \qquad (23)$$

Because creep in marble at ambient temparture was considered insig no efforts were made to derive a more exact model than the one suggested by Equation 23.

Time Dependent Failure

The time dependency of rock strength was evaluated in quasi-static compression experiments and in creep fracture tests at partial pore water pressures of 0.1 psi and 12.3 psi. Extreme variations in the strength of Westerly granite, Nugget sandstone, and Tennessee marble are listed in Table 3 as a function of test conditions.

Tests	Rock	Partial pore water pressure (psi)	Strain rate (sec^{-1})	Strength (psi)
Quasi-static compression	Westerly granite	0.1	$0(10^{-4})$	41,000
Quasi-static compression	Westerly granite	12.3	$0(10^{-5})$	33,200
Creep	Westerly granite	12.3	$\geq 10^{-11}$	25,300
Quasi-static compression	Nugget sandstone	0.1	$0(10^{-3})$	41,000
Quasi-static compression	Nugget sandstone	12.3	$0(10^{-5})$	33,400
Creep	Nugget sandstone	12.3	$\geq 10^{-10}$	19,000
Quasi-static compression	Tennessee marble	0.1	$0(10^{-4})$	17,000
Quasi-static compression	Tennessee marble	12.3	$0(10^{-5})$	15.500
Creep	Tennessee marble	12.3	$\geq 0(10^{-9})$	13,600

Table 3. Failure Times under Constant Uniaxial Compression

The data in Table 3 clearly show tnat the strength of rock is not constant. Instead it may vary considerably depending on the prevailing test conditions, on time and on the rock type considered. To evaluate the time dependent strength of rock at low stress levels, even below the stresses applied in this study, direct determination of the strength in creep fracture experiments becomes extremely time consuming and costly. To avoid this difficulty more convenient predictions schemes are needed.

The classical approach (46) suggests that the long-term rock strength can be determined by correlating and extrapolating plots of the short-term rock strength versus time or of plots of the logarithm of strength versus the logarithm of time. This has been attempted in Figures 20 and 21 using the data for water-saturated Westerly granite. Inspection of both figures immediately raises a question about their usefulness. Because of the large data scatter in Figure 20 (σ is t) it can merely be concluded that the time-to-failure of granite increases rapidly with a decrease of stress. In turn, the curve which may be fit to the data in Figure 21 ($\log\sigma$ vs. $\log t$) is too complex to be extrapolated unambiguously.

In the light of the results which we·e obtained in this investigation there might be an alternate approach to calculating long-term rock strength. The approach suggested itself from a comparison of the total creep strain ε_c' which a rock undergoes up to failure with the strain ε_q between the ascending and descending parts of the complete quasi-static stress-strain curve (Figure 8). The point is best illustrated by means of Figures 22 to 24 and Figure 8. For example, in Figure 22 the uniaxial compressive strength is plotted versus the strain ε_c' which was observed for water-saturated Westerly granite at the onset of fracture under constant uniaxial compression (triangular points). Figure 22 also shows a plot of the strain ε_q between the ascending and descending parts of the uniaxial stress strain curve for water-saturated granite. At any stress $\sigma = \sigma'$ the strain ε_q is proportional to the distance from point A to B in Figure 8. Clearly there is a strong correlation between the strains ε_c' and ε_q provided they are

measured under the same pore water pressures. Equally acceptable agreement was obtained between ε_c' and ε_q for Nugget sandstone and Tennessee marble. Because of this agreement it appears that the failure time of the rock used can now be estimated in the following manner. First the time dependent strain $\varepsilon(\sigma, t)$ is calculated by means of suitable constitutive relations. Then an estimate is obtained of the maximum strain ε_q which rock can undergo prior to failure. Finally the failure time of the rock or the strength of rock for a prescribed time interval is ascertained by solving the equation

$$\varepsilon(\sigma, t) - \varepsilon_q'(\sigma) = 0 \tag{24}$$

To check the accuracy of the above scheme to predict the time dependent strength of rock, Equations (19), (20), and (21) and Figures 22 and 23 were used to compute the failure time of water saturated granite and sandstone under constant uniaxial compression. Table 4 gives a comparison of the predicted data and of the failure times which were actually measured.

Rock (Water-saturated)	Stress (psi)	Failure Time (hr)	
		Predicted	Measured
Westerly granite	31,000	0.5	0.8
	29,000	10	10
	25,000	555	542
Nugget sandstone	25,000	0.05	0.07
	20,000	197	~150 (range 90 to 300)
	19,000	1480	~1300 (range 1250 - 1475)

Table 4. Creep Fracture Times

The agreement between experimental and predicted data is quite satisfactory (see also Figure 20). At lower stress levels, the predicted failure times are somewhat larger than the actual failure times. This result is reasonable because the constitutive Equations (19), (20), and (21) do not account for accelerated creep which tends to shorten the time to failure. Also, a more careful inspection of Figures 22 to 24 (and Figures 8 to 10) suggests that the maximum creep strain is really smaller than the predicted strain when failure takes place in long-term experiments. Hence, it is concluded that the solution of Equation 24 provides only an upper bound for the time dependent strength of rock. However, because the discrepancy between the actual and predicted failure times is small, it appears that this new approach to predict the time dependent strength of rock is promising. To establish the general usefulness of the approach, obviously further work is needed. First, the approach should be tested in confining pressure experiments. Such experiments would also determine to what extent the rock strength depends on time under more general loading conditions. Second, attempts should be made to fit the quasi-static stress-strain data to "master" curves in one or several coordinate systems which are defined by suitable transformations of the old variables stress and strain (or mean stress, volumetric strain, etc.), pore water pressure, temperature, and time. If such master curves exist, then the labor involved in determining the maximum allowable creep strain ε_q' (Equation 24) could be eliminated and the accuracy of ε_q be improved.

Fabric Changes

A study of the fabric changes in rock subjected to constant or time varying stress is of considerable interest for two reasons. Fabric changes provide a physical justification for combining the results of creep and quasi-static compression experiments to predict the time dependent strength of rock. Also, if the fabric changes are distinct enough, then they might aid the prediction of impending time dependent fracture of rock in situ.

Fabric changes in brittle rock under quasi-static loading conditions have been described extensively in the literature (7,9,17,38,39). In medium and coarse grained rock subjected to high uniaxial compression, the predominant phenomena consist of micro-cracking parallel to the applied compression, spalling and terminal shear failure (38,39). In fine grained rock, such as diabase or Solenhofen limestone, the fabric changes are much more subtle and, therefore, difficult to define. According to one school of thought, only minor fabric changes occur up to the uniaxial compressive strength which is ultimately controlled by discrete axial cleavage fracture (55). Another interpretation of experimental observations suggests that substantial micro-cracking develops already around 50% to 60% of the uniaxial compressive strength and that macroscopic failure is due to high angle faulting (37,39). The same observations indicate that micro-cracks in fine grained rocks favor orientations between 20° and 28° from the loading direction (39).

Fabric changes in rock subjected to constant uniaxial compression appear

to differ considerably depending on the range of stresses considered. However, above approximately half the quasi-static compressive strength, creep always appears to be associated with micro-cracking which was observed both directly in microscopic analyses (39,56), and indirectly by means of seismic techniques (14,36). Particularly, it was observed that the micro-crack patterns at the onset of macroscopic collapse were quite similar to the crack patterns which govern the descending branch of the complete stress-strain curve at the same stress level. This means that the fracture patterns in Westerly granite which determine its strength at, for example, point B in Figure 3 are very much alike regardless of the preceeding deformation history. It is this observation which suggested the development of a new approach to the prediction of time dependent rock strength. If micro-cracking is the controlling mechanism for creep and time dependent rock failure, then it is reasonable to postulate a one-to-one correlation between the amount of strain and the micro-crack density at any time during creep. Hence it is logical to postulate that the likelihood of impending time dependent failure could be predicted in situ if the changes of the rock fabric with time could be monitored. These changes could be measured on field samples which are collected at appropriate time intervals. Alternatively, the fabric changes could be determined indirectly by monitoring micro-seismic events or by in situ measurement of those rock properties which are sensitive to micro-crack density, for example accoustic velocity, resistivity, electrical conductivity, or permeability. Obviously, any one of these

approaches can be successful only if the micro-crack density is easily observable and if it produces substantial changes of other rock properties.

Eighteen polished sections were viewed microscopically: 1) to confirm earlier observations concerning the similarity between quasi-statically and creep induced fracture patterns, and 2) to evaluate the intensity of micro-cracking during rock creep. Comparisons of micro-crack patterns were attempted at points A, B, and C along the stress-strain paths shown in Figure 3. The observations are most conclusive for Tennessee marble. Figure 25 gives two sketches. The crack patterns in Figure 25: (a) qualitatively characterize the rock fabric after the rock was loaded to 14,000 psi and immediately unloaded again at the strain rate of approximately 10^{-5} sec.$^{-1}$. The sketch in Figure 25: (b) qualitatively defines the crack patterns which were observed at the onset of creep fracture at the same stress. The crack configurations of Figure 25: (b) are essentially identical to that found in another sample which was deformed through the quasi-static compressive strength to 14,000 psi along the descending branch of the complete stress-strain curve. Therefore, the evidence of Figure 25: (b) at least qualitatively substantiate earlier observations. It is hoped that quantitative comparisons of the three rock samples of Figure 25 can be made in the future by means of optical data processing techniques (57).

The fabric changes in Westerly granite and Nugget sandstone could not be identified as readily as in marble because both rocks were very

finely grained. The grain size of the granite used in this study was considerably smaller than the grain size of Westerly granite which was tested in an earlier investigation (39). The macroscopic events of spalling and terminal shear failure in all controlled quasi-static experiments appeared to be identical to the events recorded for other brittle rocks (38,39). They also appeared to be very similar to the terminal macroscopic fracture configurations in Westerly granite subjected to constant stress. However, the possibility exists that they differ from the terminal fracture patterns which develop during creep in Nugget sandstone. Very distinct conjugate, inclined, linear features were observed on the free surfaces of several sandstone samples at stress levels below 22,000 psi. These features are well developed in the sample of Figure 26 and resemble the "slip line" patterns in ductile metals, ductile rocks under high confining pressure but also in brittle, extremely fine grained rock such as diabase (39). Future work will have to determine whether these inclined linear features are unique for creep in sandstone at relatively low stress levels or whether they are always present and only difficult to recognize.

Little can be said about the microscopic features in granite and sandstone. The micro-crack density generally appeared to be higher in deformed samples then in undeformed "standard" specimens. The majority of micro-cracks followed grain boundaries and were not preferentially aligned. Transgranular cracks occurred predominantly parallel to the applied compression, particularly in quartz grains. Overall, optical microscopy simply did not provide the resolution needed to determined and to compare the micro-crack patterns more definitely.

PRACTICAL CONSEQUENCES OF RESULTS

The research which is described in this report was conceived to provide some new insight into the fundamental aspects of rock behavior but mainly to resolve two practically important question:

1. How significant is the time dependent behavior of rock and what might be the time dependent readjustments of stresses and strains (displacements) in rock surrounding underground or surface structures?

2. What is the long-term strength of rock and how can it be predicted?

Obviously, neither of these two questions will be answered completely until more comprehensive experiments have been conducted than could be carried out in a one-year pilot program. Nevertheless, the results of this study suggest several interesting conclusions.

The comparative behavior of Westerly granite, Nugget sandstone, and Tennessee marble in quasi-static compression and in creep experiments indicates a strong correlation between the quasi-static failure behavior and the tendency of rock to creep at ambient temperature. Rock which exhibits class I failure behavior appears to be less prone to deform with time than class II rocks irrespective of the magnitude of the pore water pressure. On the other hand, the time dependent deformations in class II rocks may be appreciable and are enhanced at elevated pore water pressure. Estimates of the possible strain accumulation in granite and sandstone were obtained by means of Equations (19) and (20)

and are listed in Table 5.

Rock	Stress (psi)	Strain (10^{-6})		
		1 year	3 years	10 years
Westerly granite	24,000	1,595		
	20,000	375	590	990
Nugget sandstone	17,000	680	1,037	2,200
	15,000	250	350	530

Table 5. Time strain accumulation in granite and sandstone.

The data in Table 5 suggest that strains up to $1,000 \times 10^{-6}$ and $2,200 \times 10^{-6}$ may develop in Westerly granite and Nugget sandstone over a ten-year period in uniaxial compression at only 20,000 psi and 17,000 psi respectively. Both strain values are much higher than was expected intuitively from measurements of the high quasi-static compressive strengths in the air-dried state, 37,500 psi for granite, and 33,400 psi for sandstone. They are appreciable if it is considered that approximately 10,000 psi must be applied to both rocks to produce "elastic" strains of the same magnitude (Figures 8 and 9).

All tests to determine the time dependent strength of granite, sandstone, and marble lead to entirely analogous conclusions. Again, a strong correlation is noted between the failure properties and the

reduction of rock rength with time. The observed decrease of the
compressive strength of Tennessee marble with an increase of loading
time and pore water pressure was less than 15%. On the other hand,
the observed strengths of Westerly granite and Nugget sandstone dropped
to 68% and 57% respectively, and are likely to decrease further as the
loading time and pore water pressure are increased. The comparative
behavior of the three rock types used here, therefore, suggests that
the long-term strength of class II rocks may lie considerably below
their quasi-static compressive strengths in the air-dried state. At
ambient temperature, the long-term strength of class I rocks appears
to be close to the quasi-static compressive strength at all pore water
pressures. The results indicate that time dependent rock failure may
well occur in certain rock formations in situ. Once failure begins,
large strains will inevitably develop. The associated displacements
in turn might increase the loads on support systems beyond their design
limits.

To predict the time dependent strength of rock, the approach
which was taken in this study appears promising in that the agreement
between predicted and measured failure times in uniaxial creep experi-
ments is quite satisfactory. However, at present the approach is
practically useful only to the extent to which laboratory strength
values can be correlated wtih the strength of rock in situ. The
approach may become more viable once the relationship between time
dependent deformations, onset of time dependent failure, and fabric

changes have been established.

A final but significant conclusion of this research pertains to the existence of class I and class II failure behavior of rock which has been questioned by numerous investigators. Class I and class II failure behavior are defined to prevail if the slope of the descending part of the complete stress-strain curve is either negative or positive (38,39). It has been purported that both types of behaviors are not inherently characteristic for rock but rather are merely a consequence of certain experimental conditions. If this were true, then it might be expected that the strain to failure in creep experiments at some stress $\sigma < \sigma_c$, i.e., the sum of the "instantaneous" and the creep strains, would be greater than the strain ε_c which is associated with quasi-static uniaxial compressive strength σ_c. This condition did not develop in any of the creep experiments which were carried out on Westerly granite and Nugget sandstone. On the contrary, class II post-failure was reached along a new and entirely different path. The existence of class II failure behavior was therefore confirmed in an independent experiment. Similarly, if the occurrence of class I failure behavior depended on the experimental conditions used, then "class I rocks" might exhibit "class II" behavior in creep. This condition did not arise in Tennessee marble. Instead, all experimental evidence suggests that the sum of the instantaneous and of the creep strains are always greater than the strain ε_c.

REFERENCES

1. Michelson, A. A., "The Laws of Elastico-Viscous Flow," J. Geol., 47, 3, 1939.

2. Griggs, D. T., "Deformation of Rocks Under High Confining Pressure," J. Geol., 44, 5, 1936.

3. Griggs, D. T., "Creep of Rocks," J. Geol., 47, 3, 1939.

4. Phillips, D. W., "Tectonics of Mining," Colliery Eng., XXV, 1948.

5. Lomnitz, C., "Creep Measurements in Ignious Rocks," J. Geol., 64, 5, 1956.

6. Hardy, H. R., "Time Dependent Deformation and Failure of Geologic Materials," Colorado School of Mines, Quart., 54, 1959.

7. Robertson, E. G., "Creep of Solenhofen Limestone Under Moderate Hydrostatic Confining Pressure," Geol. Soc. Am. Mem., 79, 1960.

8. Matsushima, S., "On the Flow and Fracture of Rocks," Bull. Disast. Prev. Res., Inst., Kyoto Univ., 36, 1, 1960.

9. Robertson, E. G., "Viscoelasticity of Rocks," State of the Earth's Crust, Am. Elsencir Publ. Co., 1964.

10. Misra, A. K., and Murrell, S. A., "An Experimental Study of the Effect of Temperature and Stress on the Creep of Rocks," Geophys. J. R. Astr. Soc., 9, 509, 1965.

11. LeComte, P., "Creep in Rock Salt," J. Geol., 72, 469, 1965.

12. Dreyer, W., Die Festigkeitseigenschaften natuerlicher Gesteine, insbesondere der Salz- und Karbongesteine, Clausthaler Hefte, Heft 5, Verlag Gebrueder Borntraeger, Goslar, Germany, 1967.

13. Rummel, F., "Untersuchungen der zeitabhaengigen Verformung einiger Granit- und Eklogit-Gesteinsproben unter einachsiger konstanter Druckspannung und Temperaturen bis 400°C," PhD thesis, University of Munich, Germany, 1967.

14. Scholz, C. H. "Mechanism of Creep in Brittle Rock," J. Geophys., Res. 73, 10, 1968.

15. Cruden, D. M., "Creep Law for Rock Under Uniaxial Compression," <u>Int. J. Rock Mech. Min. Sci.</u>, 8, 2, 1971.

16. Cruden, D. M. "Single Increment Creep Experiments on Rock Under Uniaxial Compression," ibid.

17. Heard, H. C., "The Effects of Large Changes of Strain Rate in the Experimental Deformation of Rock," <u>J. Geol.</u>, 71, 2, 1963.

18. Simpson, D. R., and Fergus, J. H., "The Effect of Water on the Compressive Strength of Diabase,"

19. Krokosky, E. M. and Husak, A., "Strength Characteristics of Basalt-Like Rock in Ultra-High Vacuum," <u>J. Geophys. Res.</u>, 73, 6, 1968.

20. Colback, P. S. B., and Wiid, B. L., "The Influence of Moisture Content on the Compressive Strength of Rock," Rock Mech. Symp. University of Toronto, 1965.

21. Scholz, C. H., personal communication, 1971

22. Martin, R. J. III, "Time Dependent Crack Growth in Quartz," <u>Trans. Am. Geophys. Union</u>, 52, 4, 1971.

23. Glathart, J. R., and Preston, F. W., "Fatigue Models in Glass," <u>J. Appl. Phys</u>, 17, 3, 1946.

24. Charles, R. J., "The Strength of Silicate Glasses and Some Crystalline Oxides," Proc Intern. Conf. on Fracture, MIT Press, 1959.

25. LeRoux, H., "The Strength of Fused Quartz in Water Vapor," <u>Proc. Poy. Soc. London</u>, A 286, 390, 1965.

26. Brace, W. F., and Martin, III, "A Test of the Law of Effective Stress for Crystalline Rocks of Low Porosity," <u>Int. J. Rock Mech. Min. Sci.</u>, 5, 2, 1968.

27. Cornet, F. H., "The Effect of Pore Fluid on the Mechanical Behavior of Rocks," Proc. 13th Symp. Rock Mech., University of Illinois, 1971.

28. Serdengecti, S., and Boozer, G. D., "The Effect of Strain Rate and Temperature on the Behavior of Rocks Subjected to Triaxial Compression," Min. Ind. Exp. Sta. Bull., Penn. State Univ., 76, 1961.

29. Price, N. J., "A Study of Time-Strain Behavior in Coal Measure Rocks," <u>Inv. J. Rock Mech. Min. Sci.</u>, 1, 2, 1964.

30. Green, S. J., and Perkins, R. D., "Uniaxial Compression Tests at Strain Rates from 10^{-4}/sec. to 10^4/sec on Three Geological Materials," General Motors Corp., Report MSL-68-6, 1968.

31. Baker, J., and Preston, F. W., "Fatigue of Glass Under Static Loads," J. Appl. Phys., 17, 1946.

32. Odgwrist, F. K. G., "On Theories of Creep Fracture," VIII Inv. Congr. Appl. Mech., Istanbul, 1962.

33. Bieniawski, T. Z., "Mechanism of Brittle Fracture of Rock," Int. J. Rock Mech. Min. Sci., 4, 4, 1967.

34. Brace, W. F. Paulding, B. W., and Scholz, C. H., "Dilantancy in the Fracture of Crystalline Rocks," J. Geophys. Res., 71, 16, 1966.

35. Mogi, K., "Study of Elastic Shocks Caused by the Fracture of Heterogeneous Material and its Relation to Earthquake Phenomena," Bull. Earthquake Res. Instit., Tokyo University, 40, 1962.

36. Duvall, W. I., and Obert, L., "Microseismic Method of Predicting Rock Failure in Underground Mining," U. S. Bur. Mines, Dept. Inv. 3797, 1942.

37. Scholz, C. H., "Microfracturing and the Inelastic Deformation of Rock in Compression," J. Geophys., 73, 4, 1968.

38. Wawersik. W. R., "A Study of Brittle Rock Fracture in Laboratory Compression Experiments," Int. J. Rock Mech. Min. Sci., 7, 4, 1970.

39. Wawersik, W. R., and Brace, W. F., "Post-Failure Behavior of a Granite and Diabase," Rock Mech., 3, 3, 1971.

40. Hult, J., Creep in Engineering Structures, Blaisdell Publ. Co., 1966.

41. Mendelson, A., "Plasticity: Theory and Applications, MacMillan Co., 1968.

42. Conrad, H., "Experimental Evaluation of Creep and Stress Rupture," Mech. Behavior at Elevated Temperatures, J. E. Dorn, ed., McGraw-Hill, 1961.

43. Baer, E., ed., Engineering Design for Plastics, Reinhold Book Co., 1964.

44. Fitzgerald, J. E., and Hufferd, W. L., Handbook for the Engineering Structural Analysis of Solid Propellants, in press.

45. Bland, D. R., The Theory of Linear Viscoelasticity, Pergamon Press, 1960.

46. Nadai, A., Theory of Fracture and Flow of Solids, Vol. 2, McGraw-Hill, 1963.

47. Flügge, W., Viscoelasticity, Blaisdell Publ. Co., 1967.

48. Ferry, J. D., Viscoelastic Properties of Polymers, John Wiley and Sons, Inc., 1970.

49. Christensen, R. M., Theory of Viscoelasticity, Academic Press, 1971.

50. Goetze, C., "High Temperature Theology of Westerly Granite," J. Geophys. Res., 76, 5, 1971.

51. Brady, B. T., "A Mechanical Equation of State for Brittle Rock. Part I - The Pre-Failure Behavior of Brittle Rock," Int. J. Rock Mech. Min. Sci., 7, 4, 1970.

52. Smith, T. L., "Ultimate Tensile Properties of Elastomers. I. Characterization by a Time and Temperature Independent Failure Envelope," J. Polymer Sci., Part A, 1, 12, 1963.

53. Brace, W. F., "Brittle Fracture of Rocks," State of the Earth's Crust, W. R. Judd, ed., Am. Elsencir Publ. Co., 1964.

54. Brown, W. S. and Swanson, S. R., "Stress-Strain and Fracture Properties of Nugget Sandstone," UTEC ME 71-058, University of Utah, 1971.

55. Seldenrath, T. R. and Gramberg, J., "Stress-Strain Relations and Breakage of Rock," Mechanical Properties of Non-Metallic Brittle Materials, W. H. Walton, ed., Buttersworth Sci. Publ. Co., 1958.

56. Wawersik, W. R., "Detailed Analysis of Rock Failure in Laboratory Compression Tests," Ph.D. Thesis, University of Minnesota, 1968.

57. Pincus, H. J., "Optical Processing of Rectorial Rock Fabric Data," Proc. First Congr. Int. Soc. Rock. Mech., Lisbon, 1966.
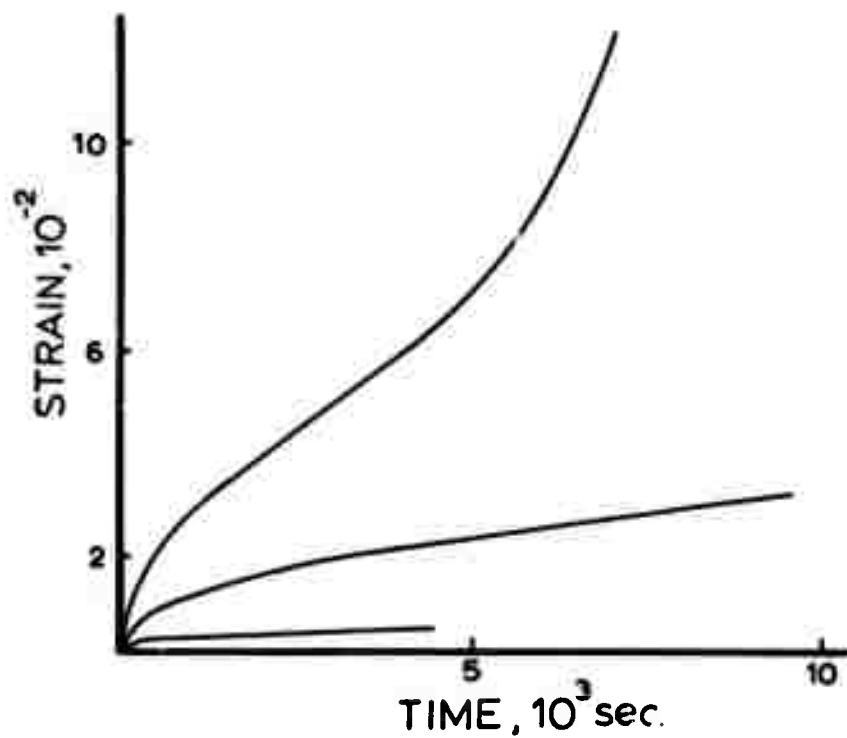
FIGURE 1. Creep curves of Solenhofen limestone subjected to different shear stresses at 150,000 psi confining pressure (after Griggs)
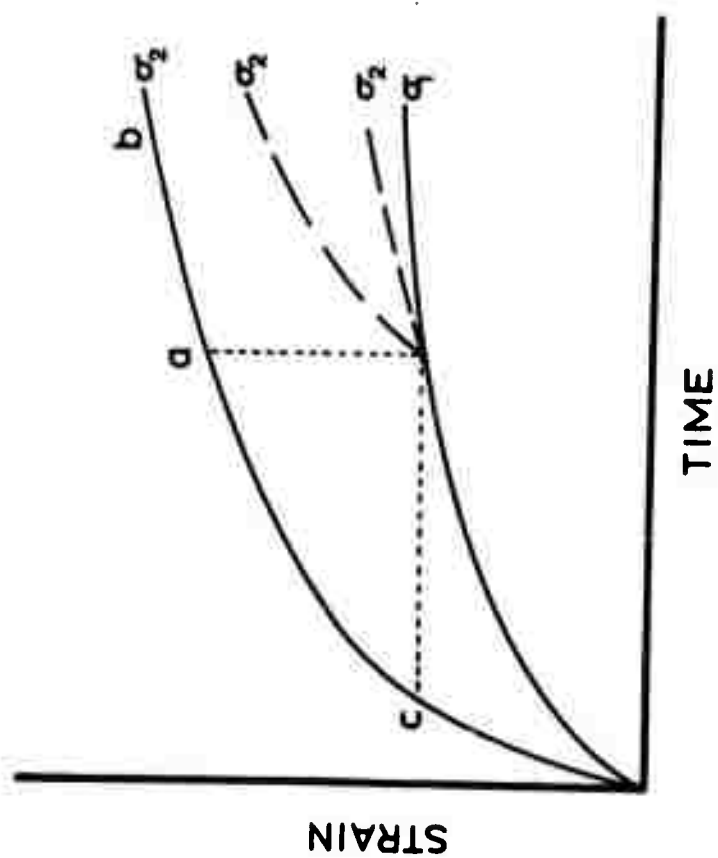
FIGURE 2. Hypothetical creep curves of rock as a function of stress
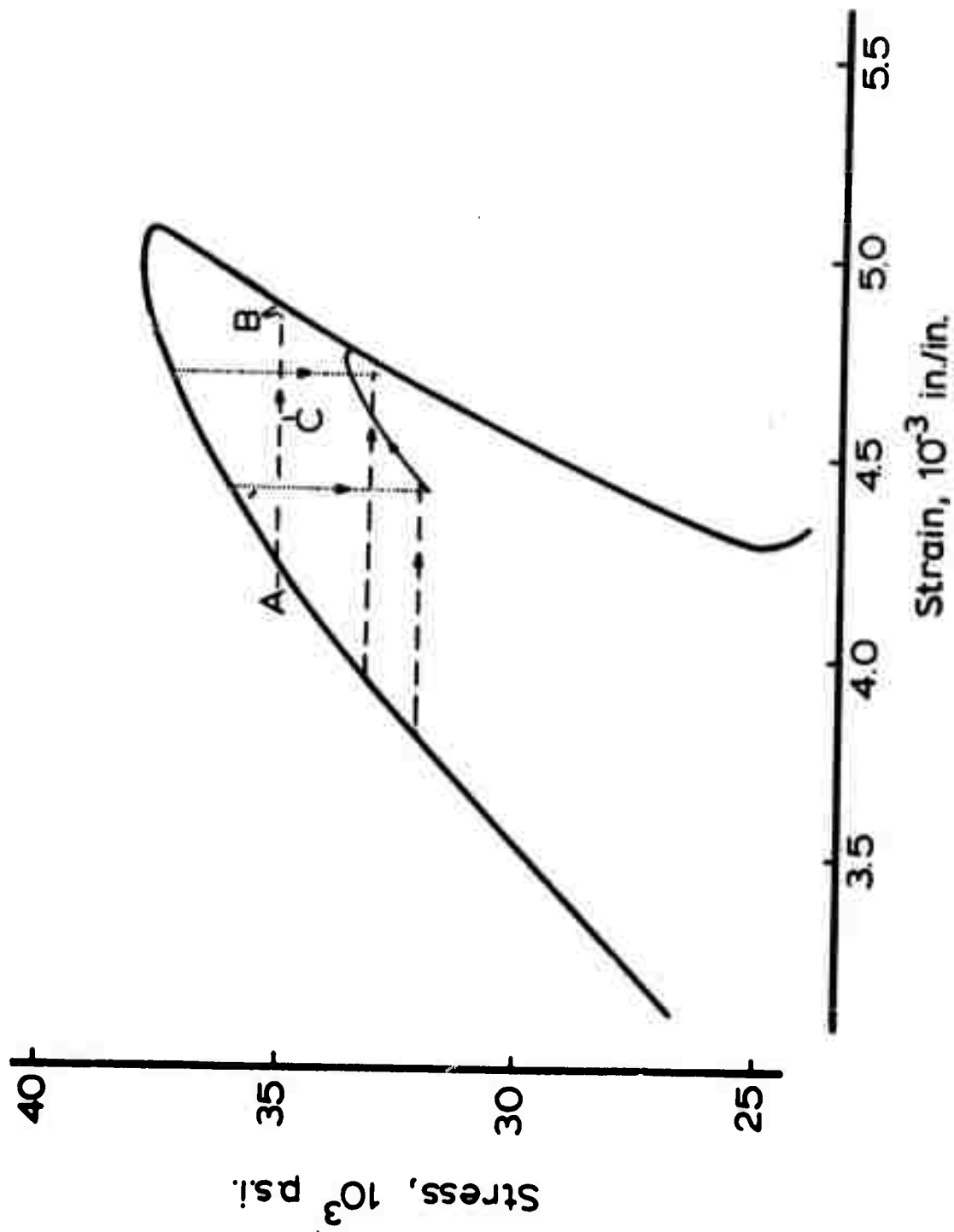
FIGURE 3. Uniaxial stress-strain behavior of Westerly granite as a function of loading history (solid lines: continuous deformation at $0(10^{-5})$ sec^{-1}; dashed lines: strain at constant load; dotted lines: stress at constant displacement) (after W. R. Wawersik and W. F. Brace, 39)
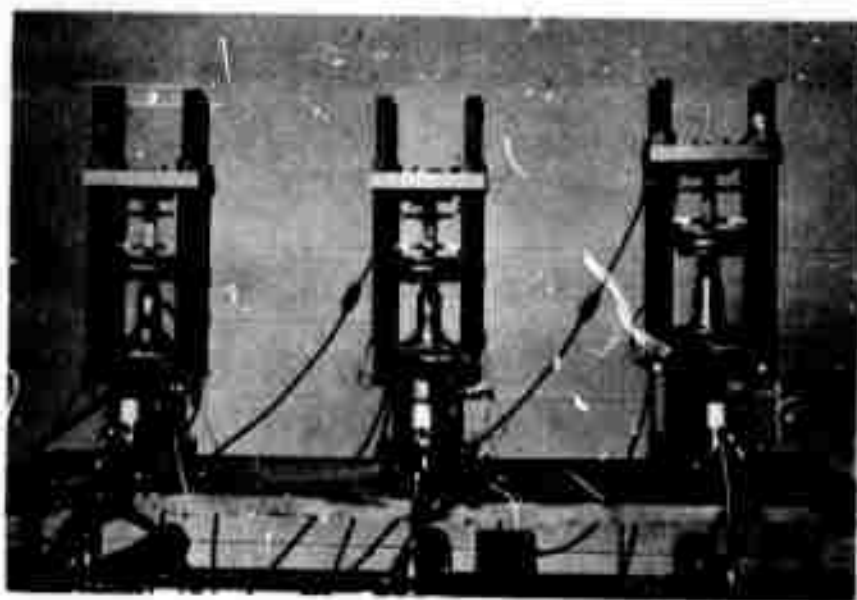
FIGURE 4. Loading apparatus

FIGURE 5. Instrumentation and data
acquisition systems
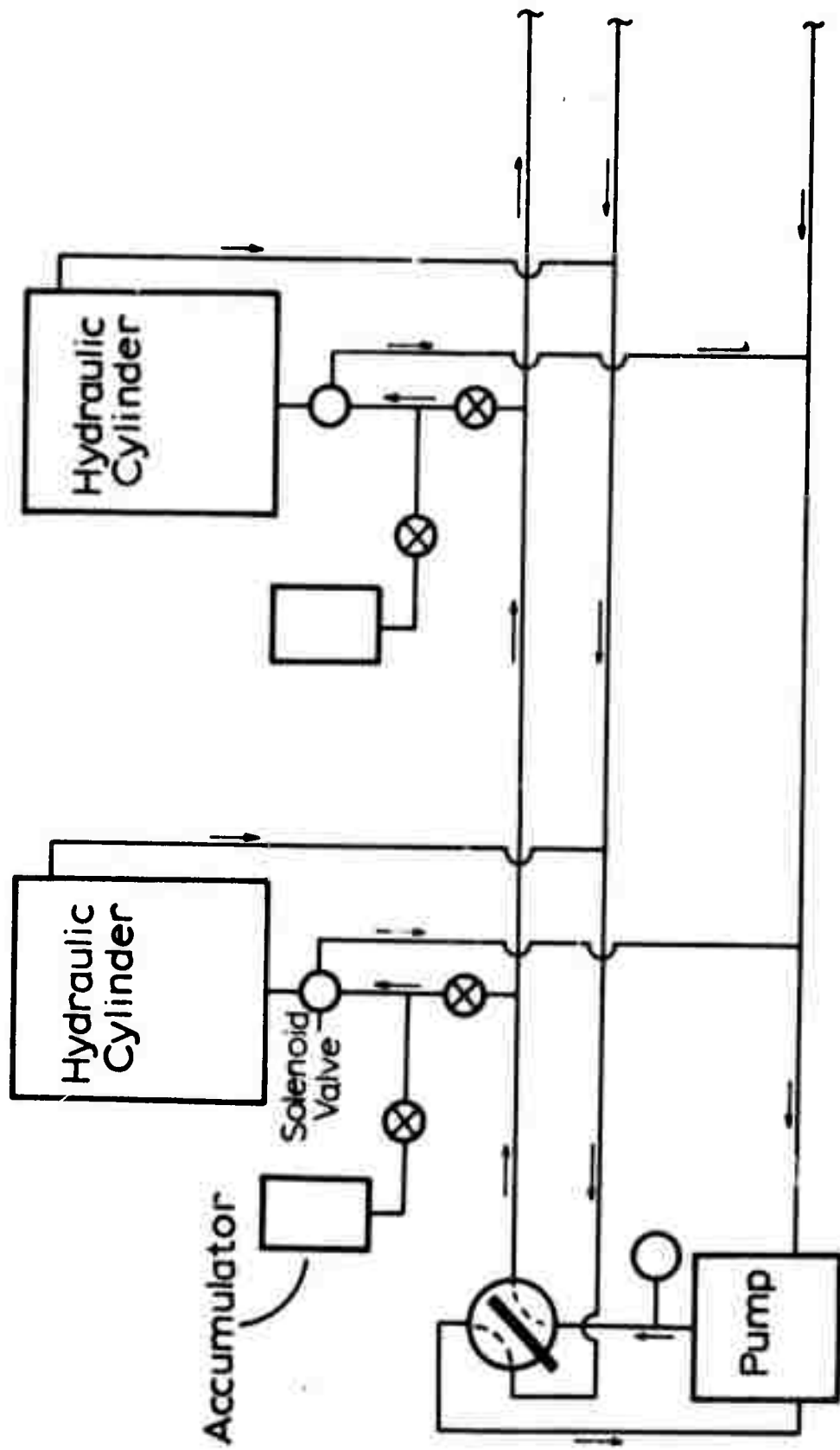
FIGURE 6.   Schematic of creep testing apparatus
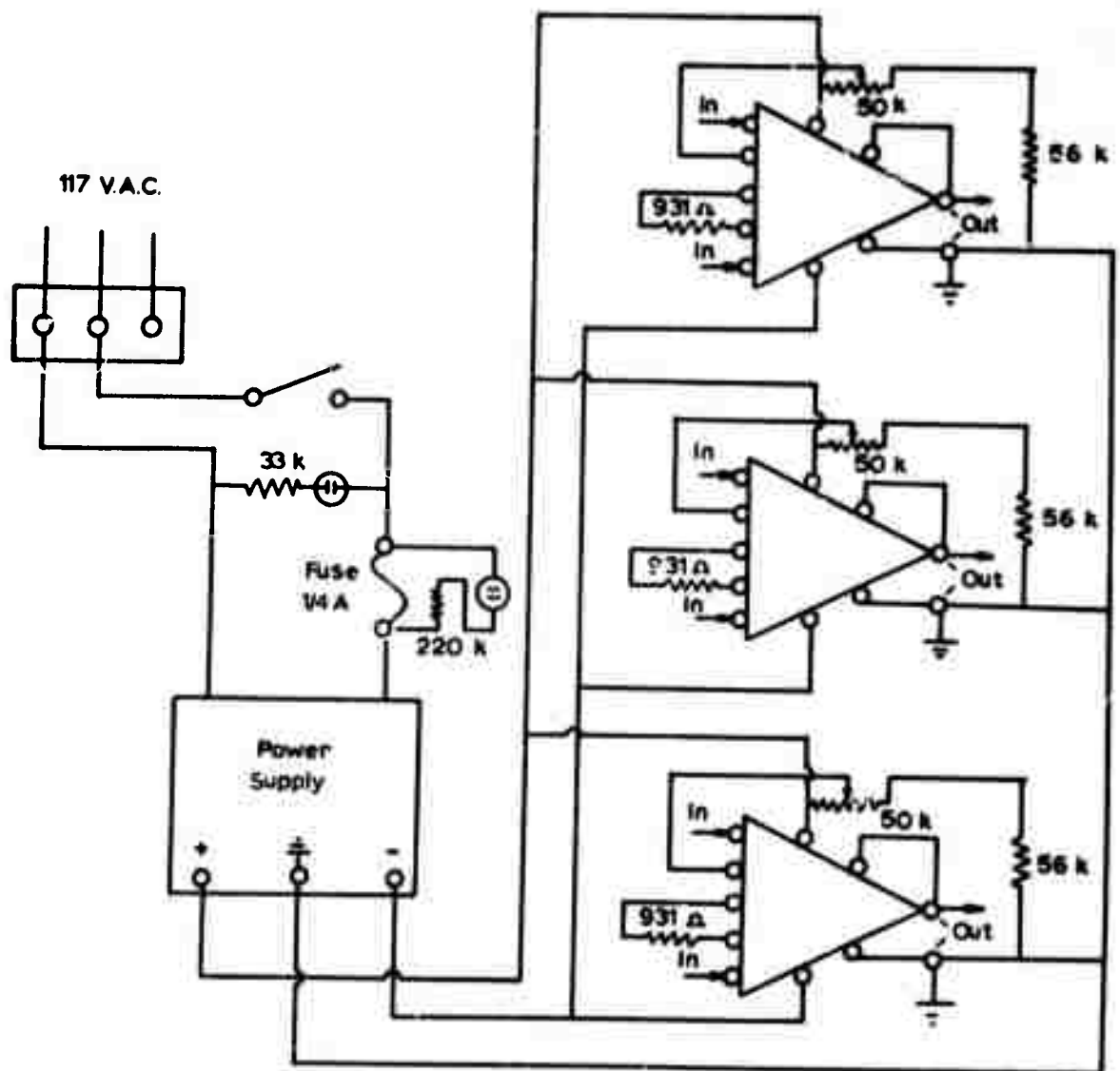
FIGURE 7. Schematic of summing circuits
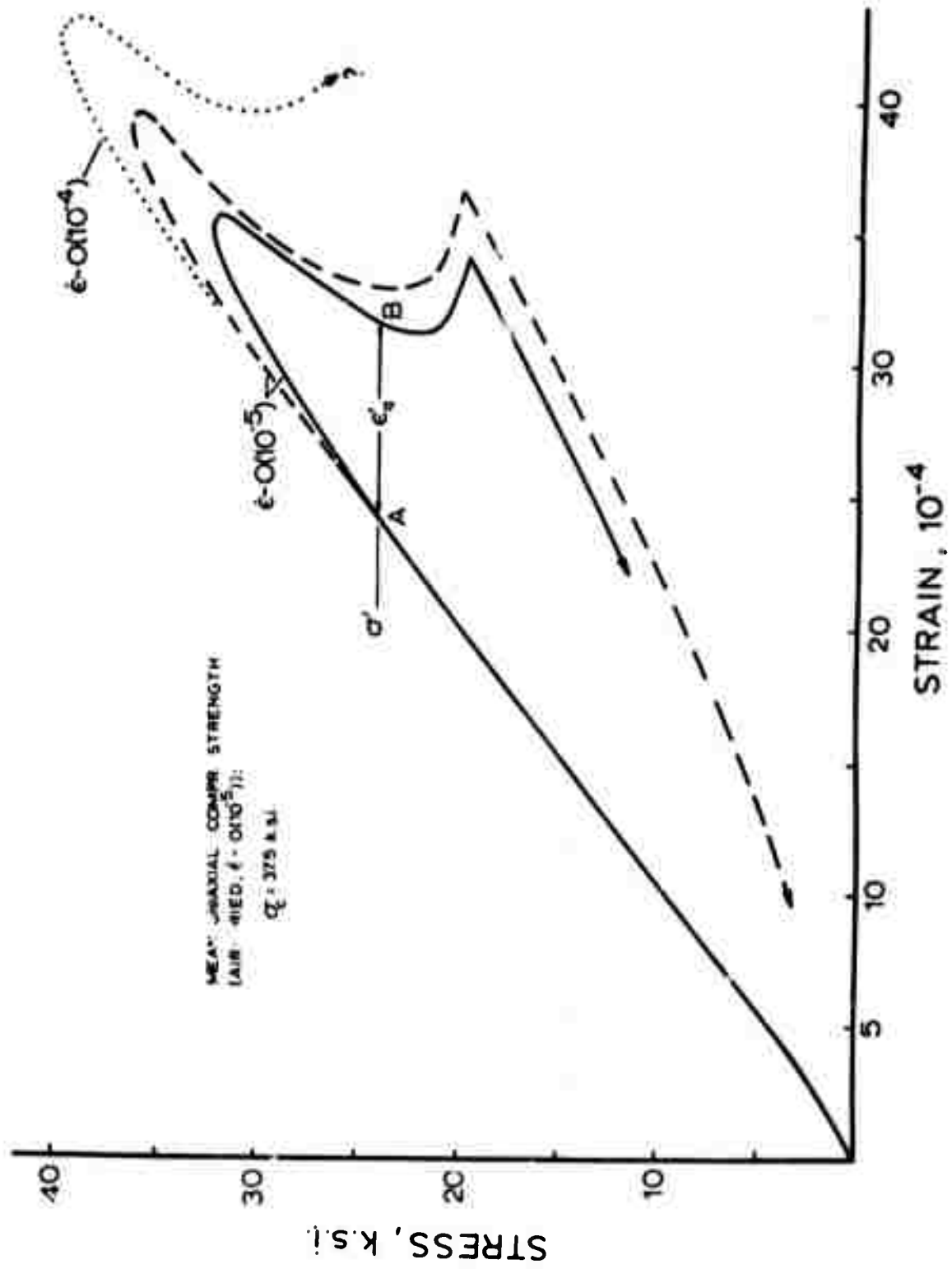
FIGURE 8. Complete quasi-static stress-strain curve of Westerly granite under uniaxial compression (solid line: water-saturated; dashed and dotted lines: air-dry)
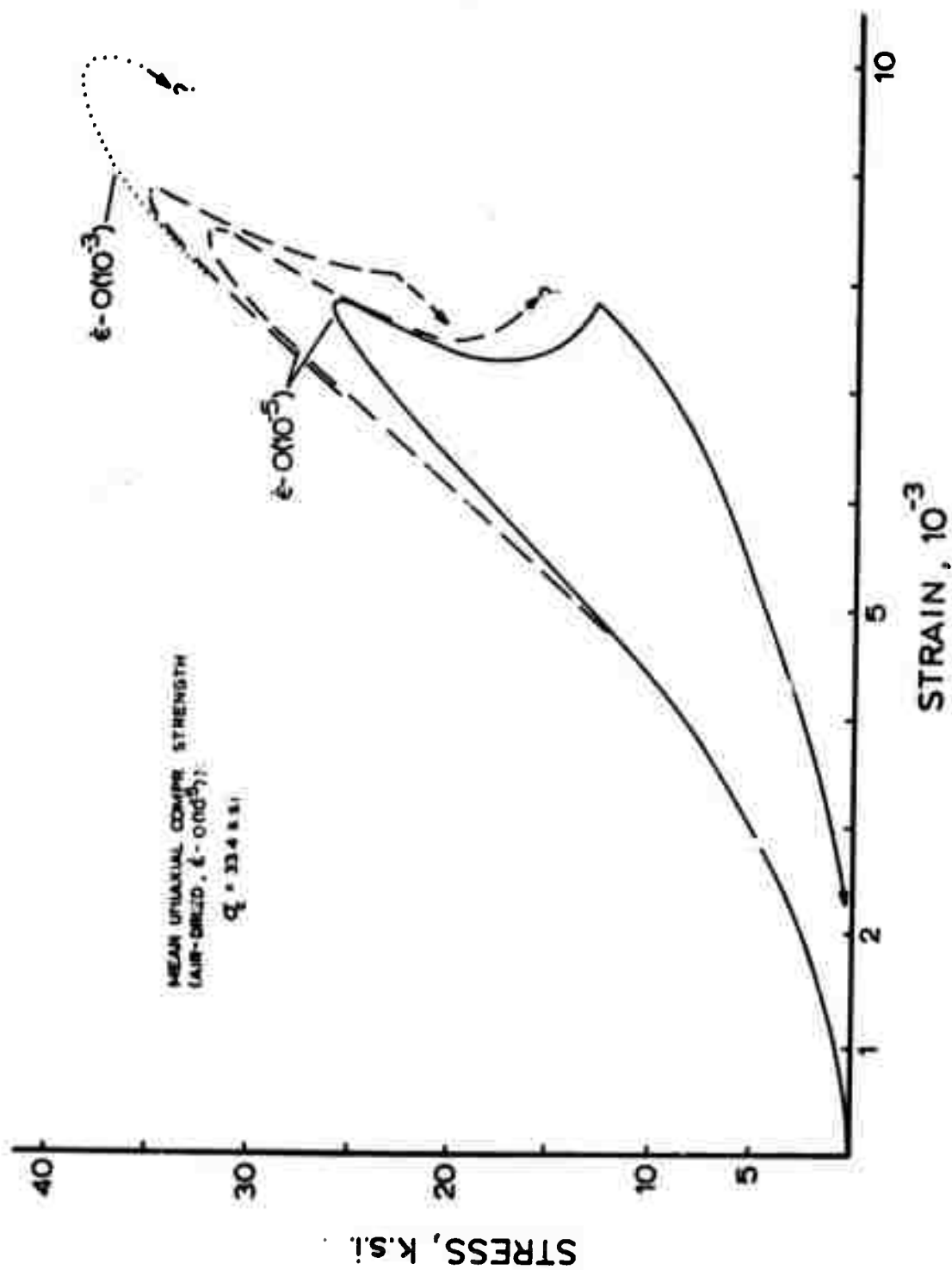
FIGURE 9. Complete quasi-static stress-strain curves of Nugget sandstone under uniaxial compression (solid line: water-saturated; dashed and dotted lines: air-dry)
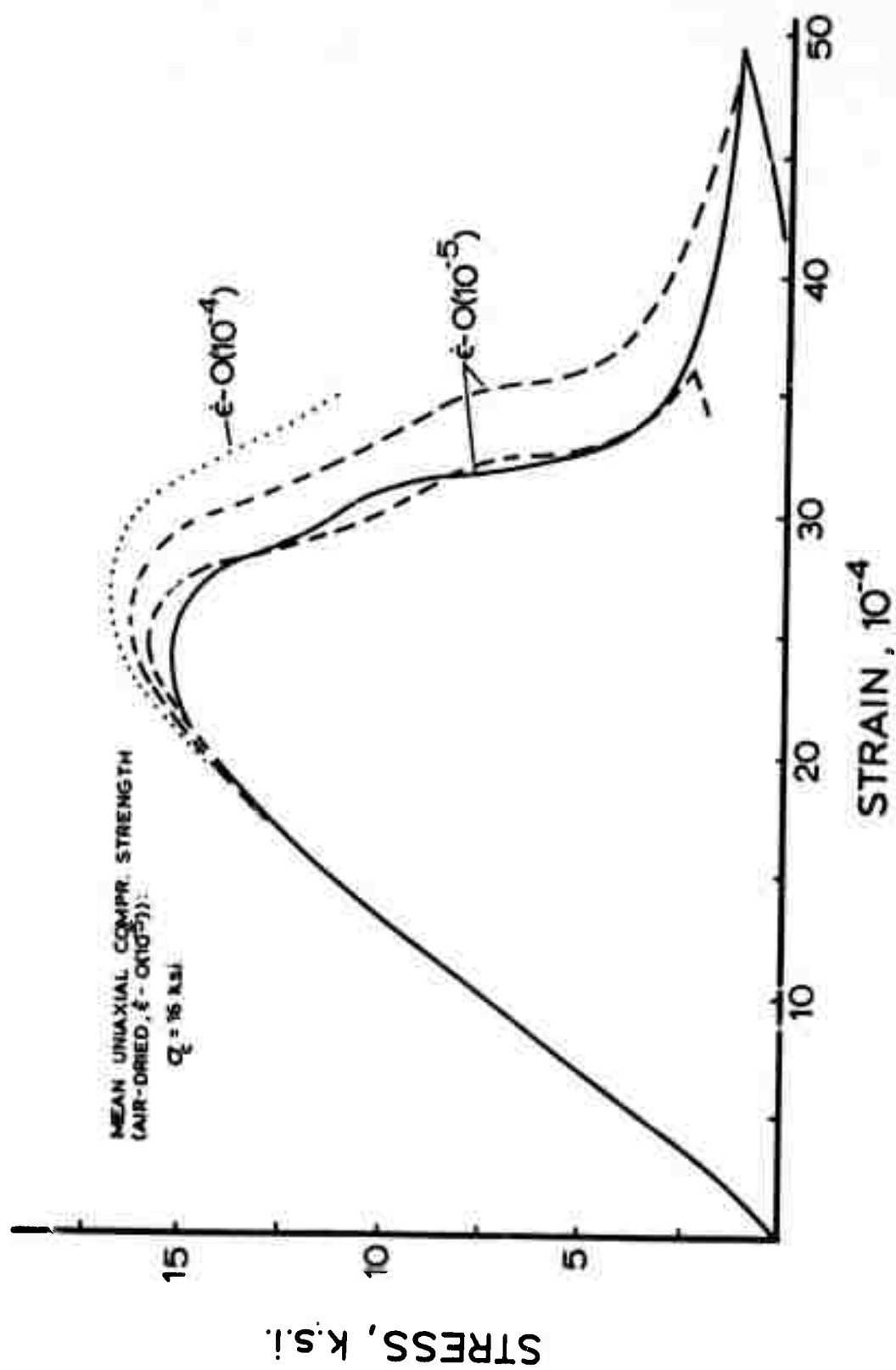
FIGURE 10. Complete quasi-static stress-strain curves of Tennessee marble under uniaxial compression (solid line: water-saturated; dashed and dotted lines: air-dry)
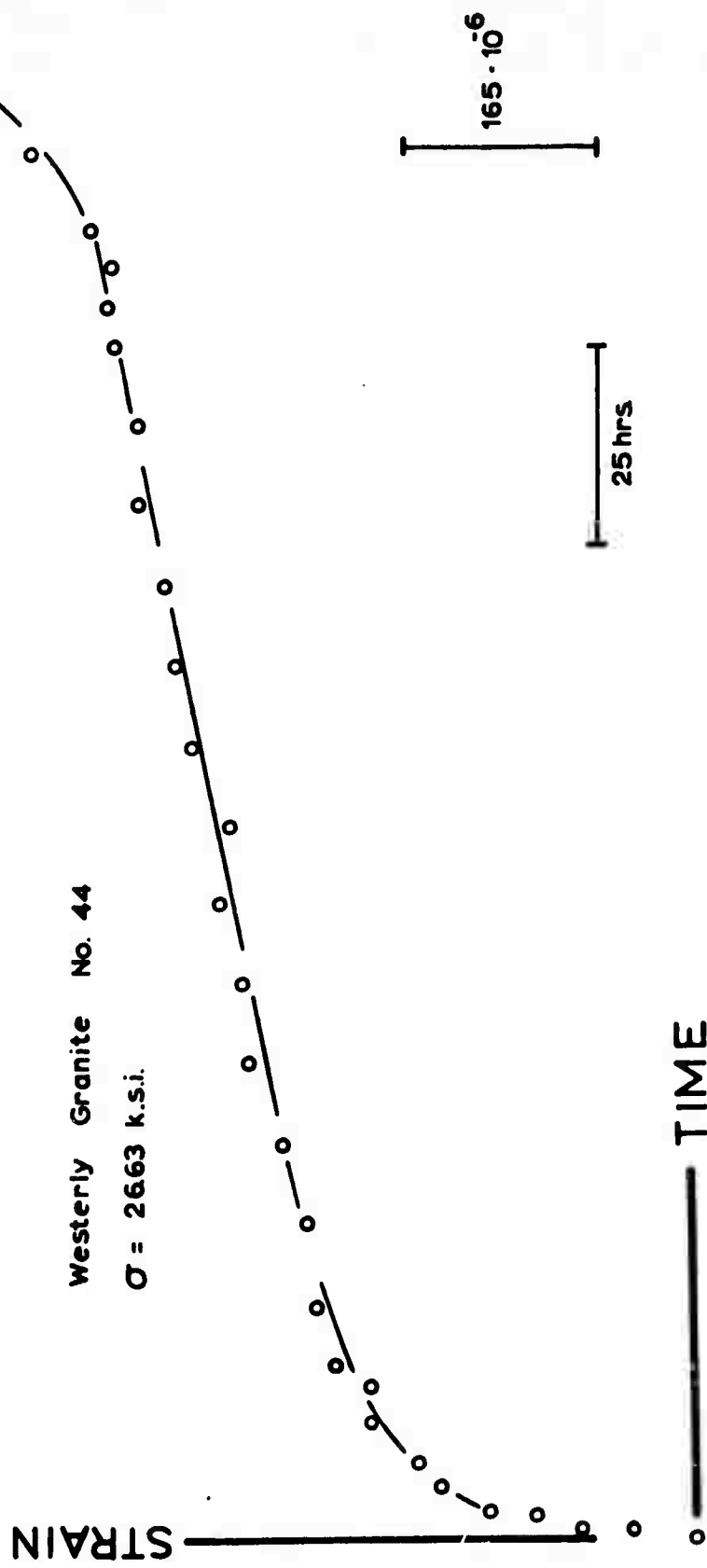
FIGURE 11. Typical creep curve of water-saturated Westerly granite
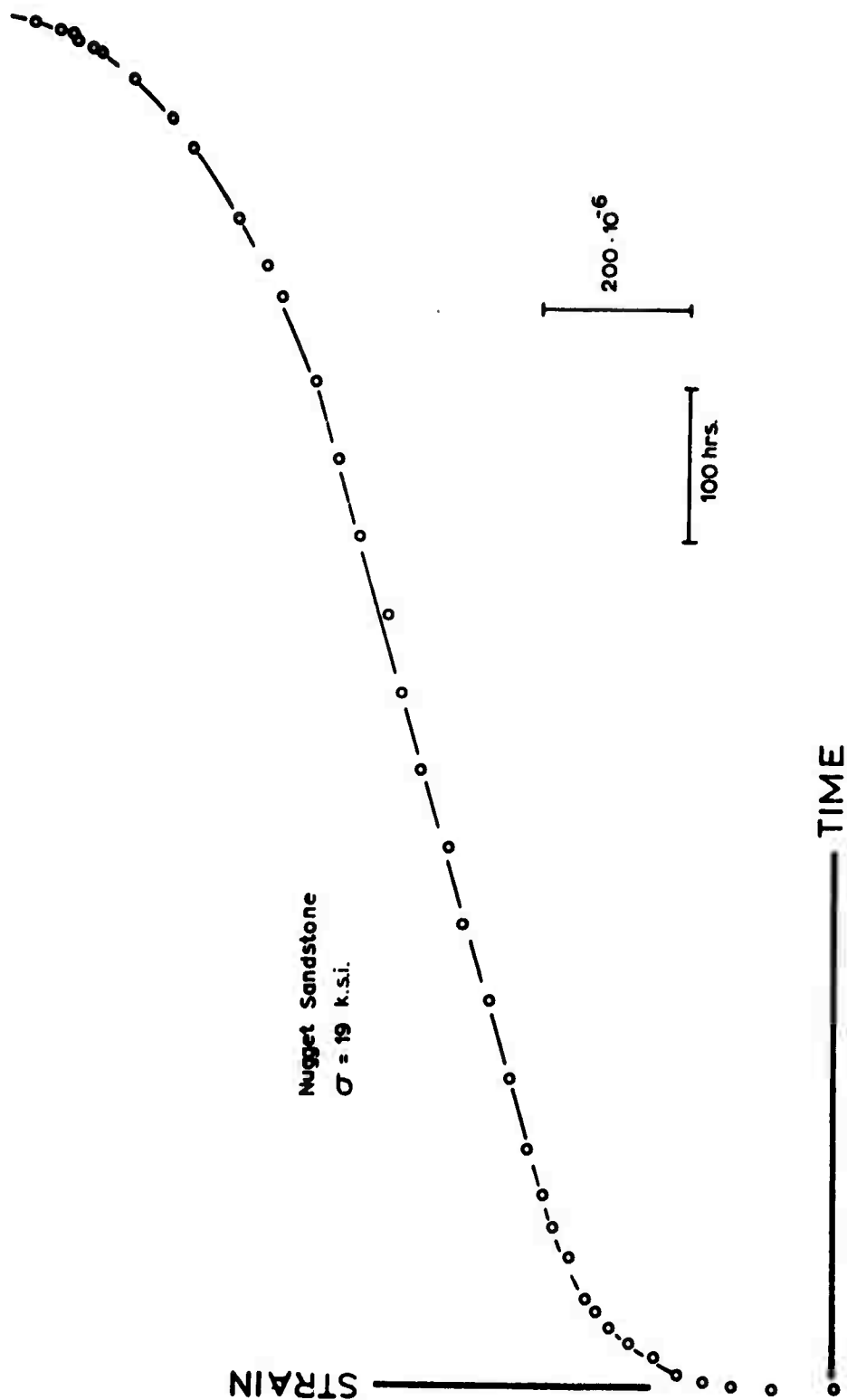
FIGURE 12. Typical creep curve of water-saturated Nugget sandstone
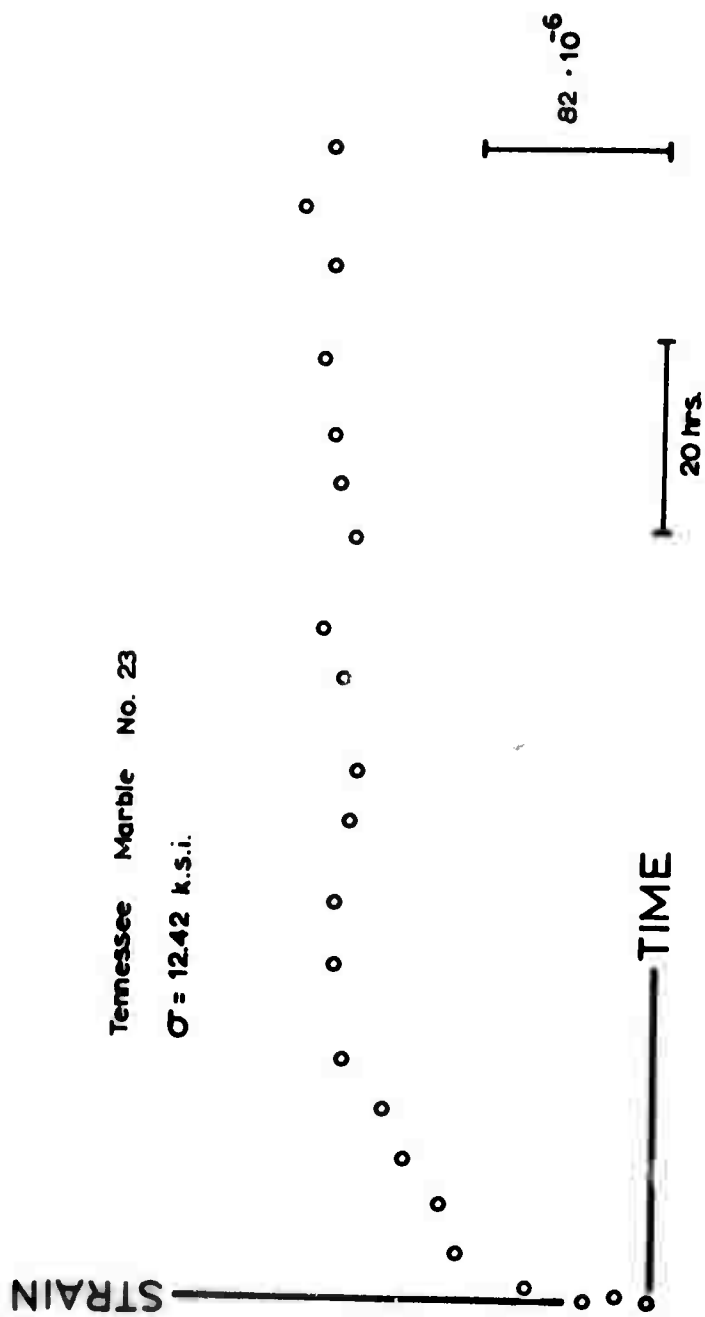
FIGURE 13. Typical creep curve of Tennessee marble
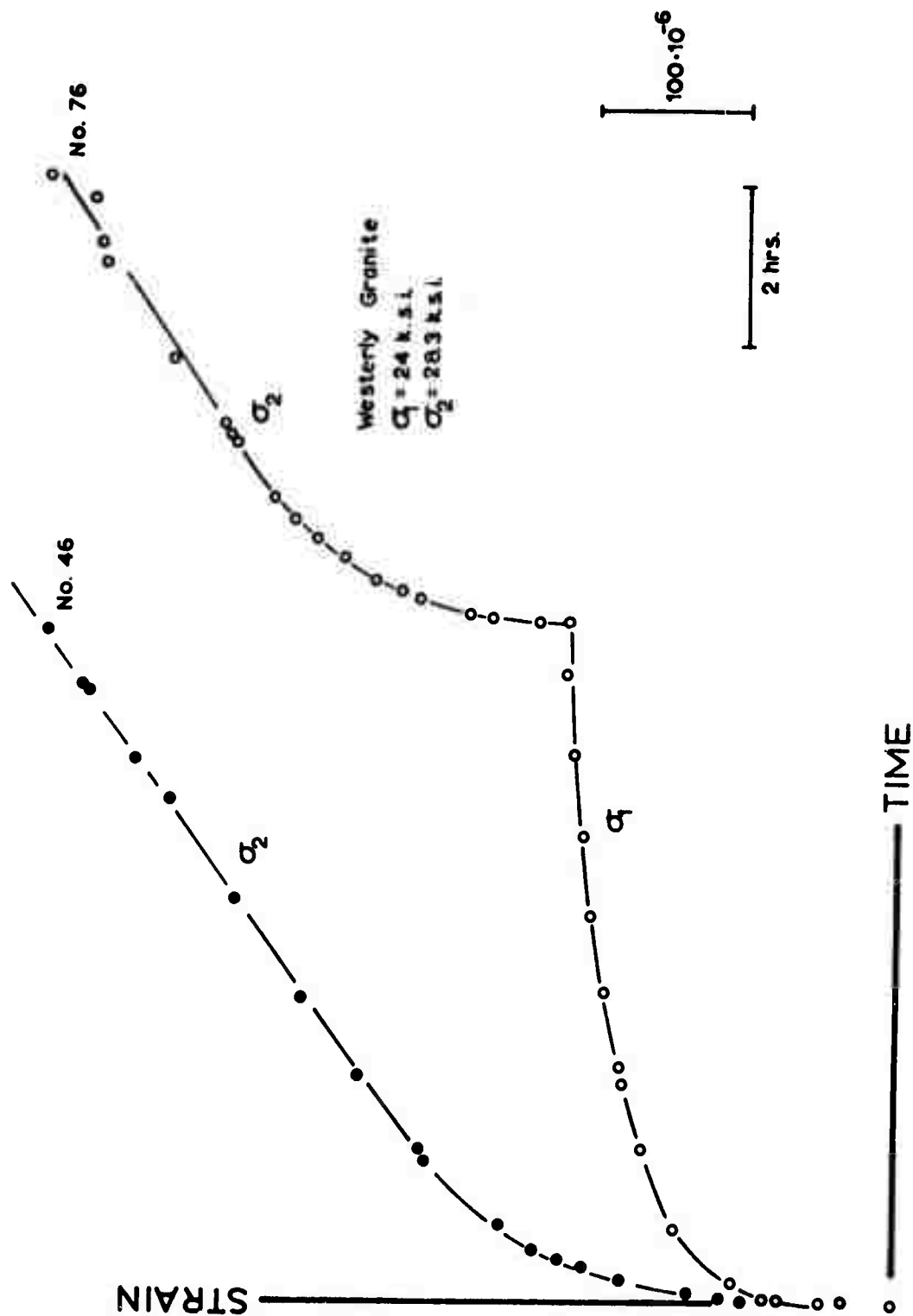
FIGURE 14. Typical creep curve of water-saturated Westerly granite subjected to differential loading
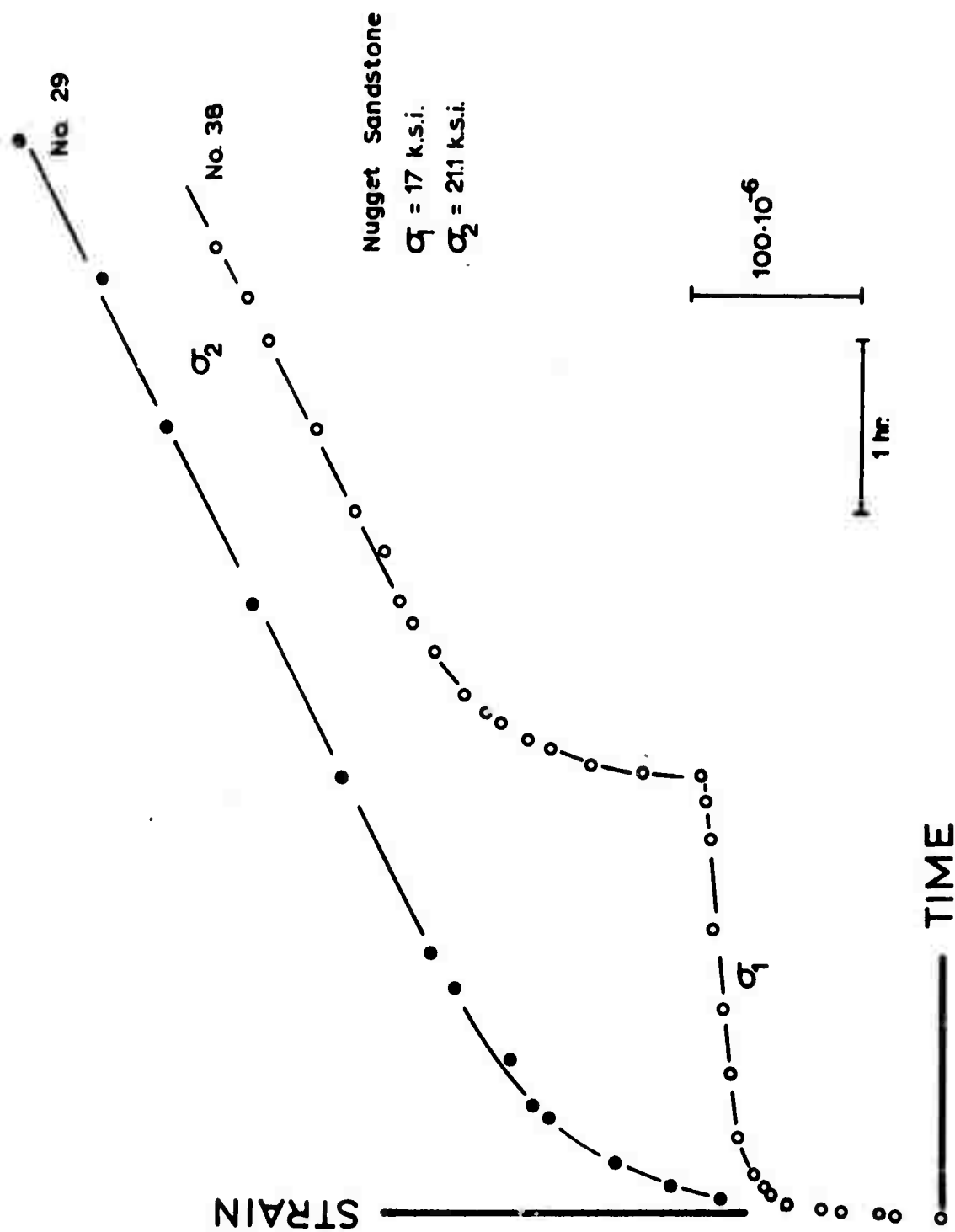
FIGURE 15. Typical creep curve of water-saturated Nugget sandstone subjected to differential loading
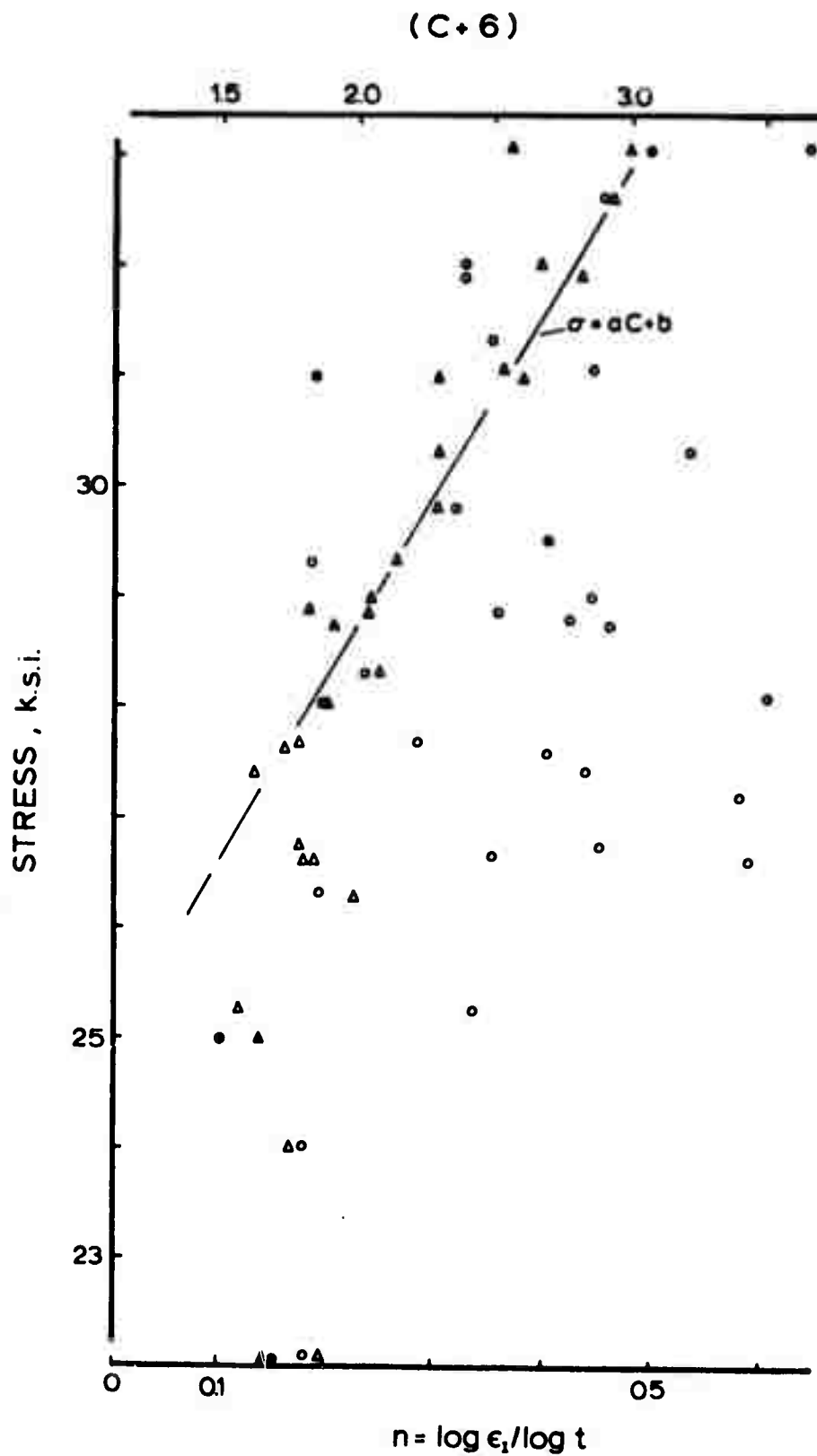
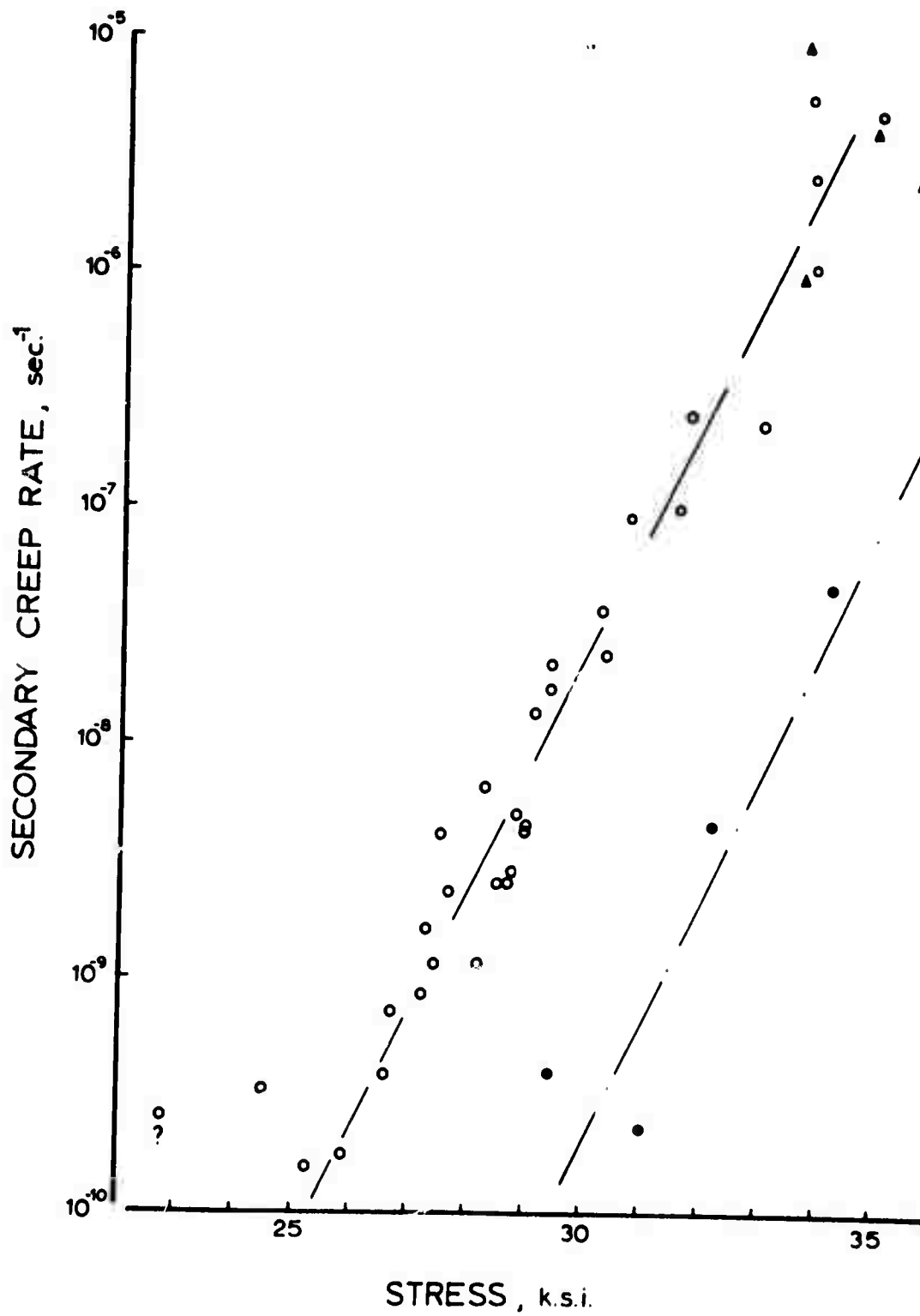FIGURE 16. Creep properties of Westerly granite during primary creep (circles: σ vs. n; triangles: σ vs. c; open symbols: water-saturated; solid symbols: air-dry)

FIGURE 17. Creep properties of Westerly granite during secondary creep (open symbols: water-saturated; solid symbols: air-dry)
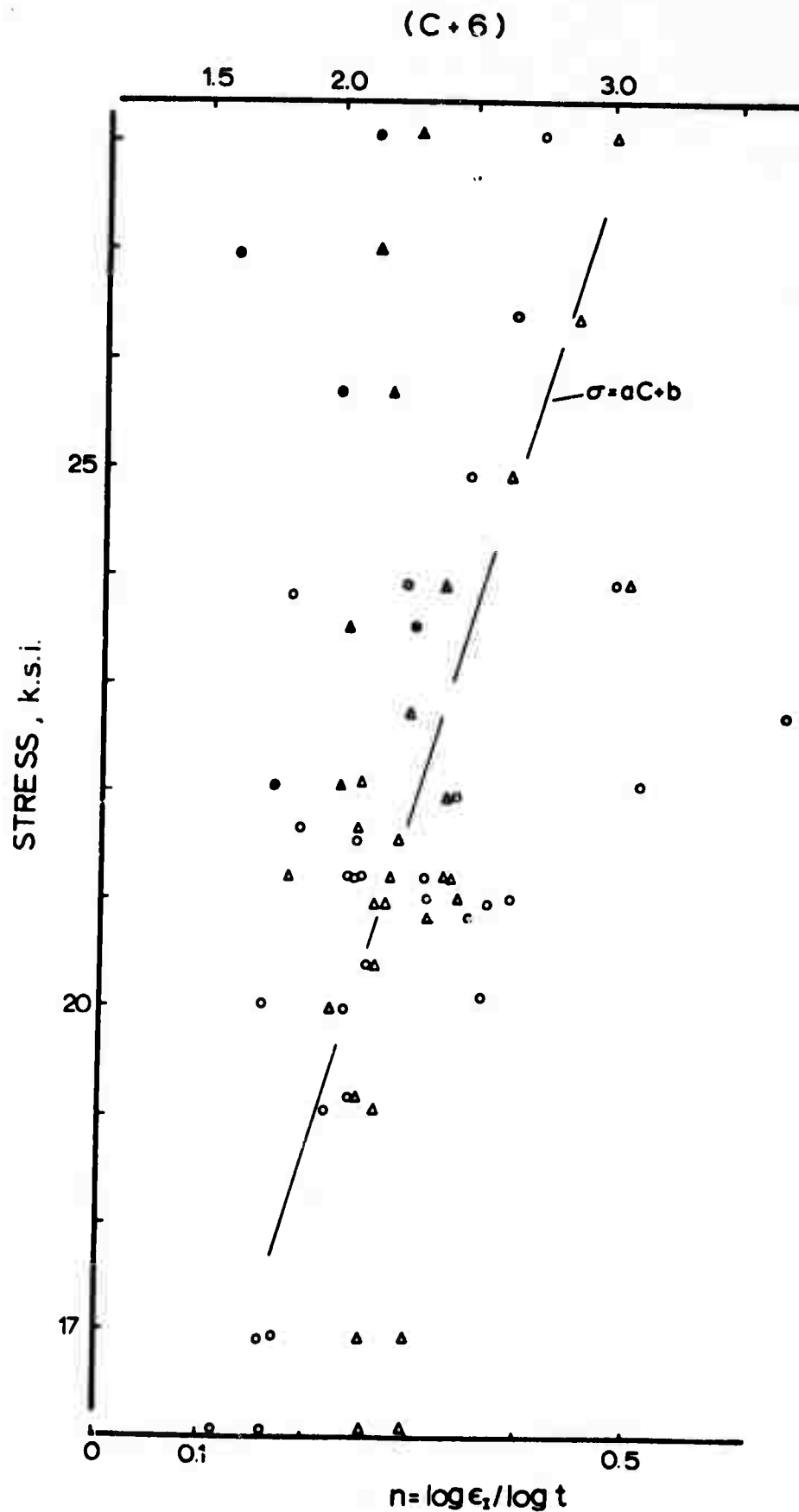
FIGURE 18. Creep properties of Nugget sandstone during primary creep (circles: σ vs. n; triangles: σ vs. c; open symbols: water-saturated; solid symbols: air-dry)
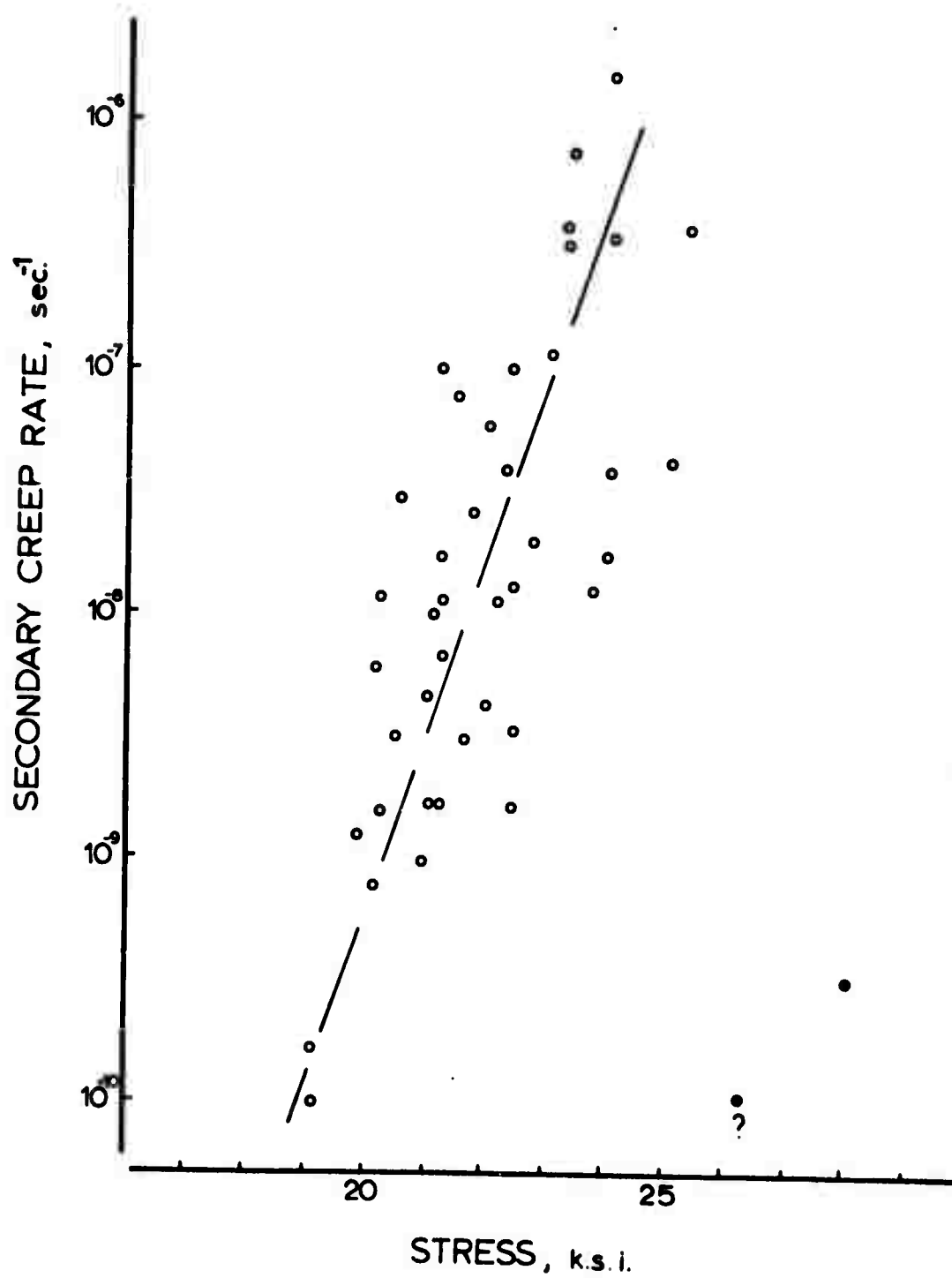
FIGURE 19. Creep properties of Nugget sandstone during secondary creep
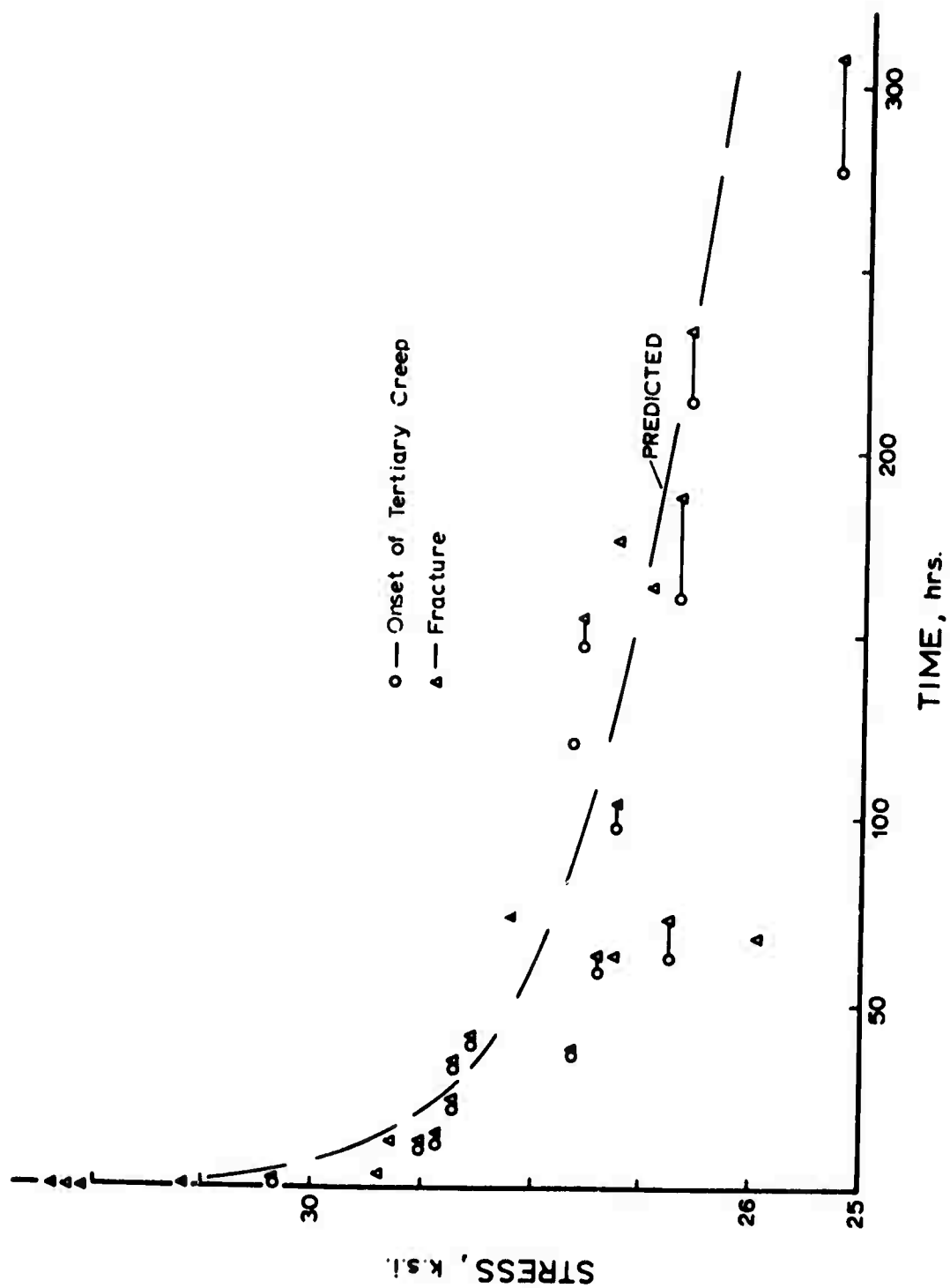(open symbols: water-saturated; solid symbols: air-dry)

FIGURE 20. Strength-time relationship for Westerly granite (σ versus t)
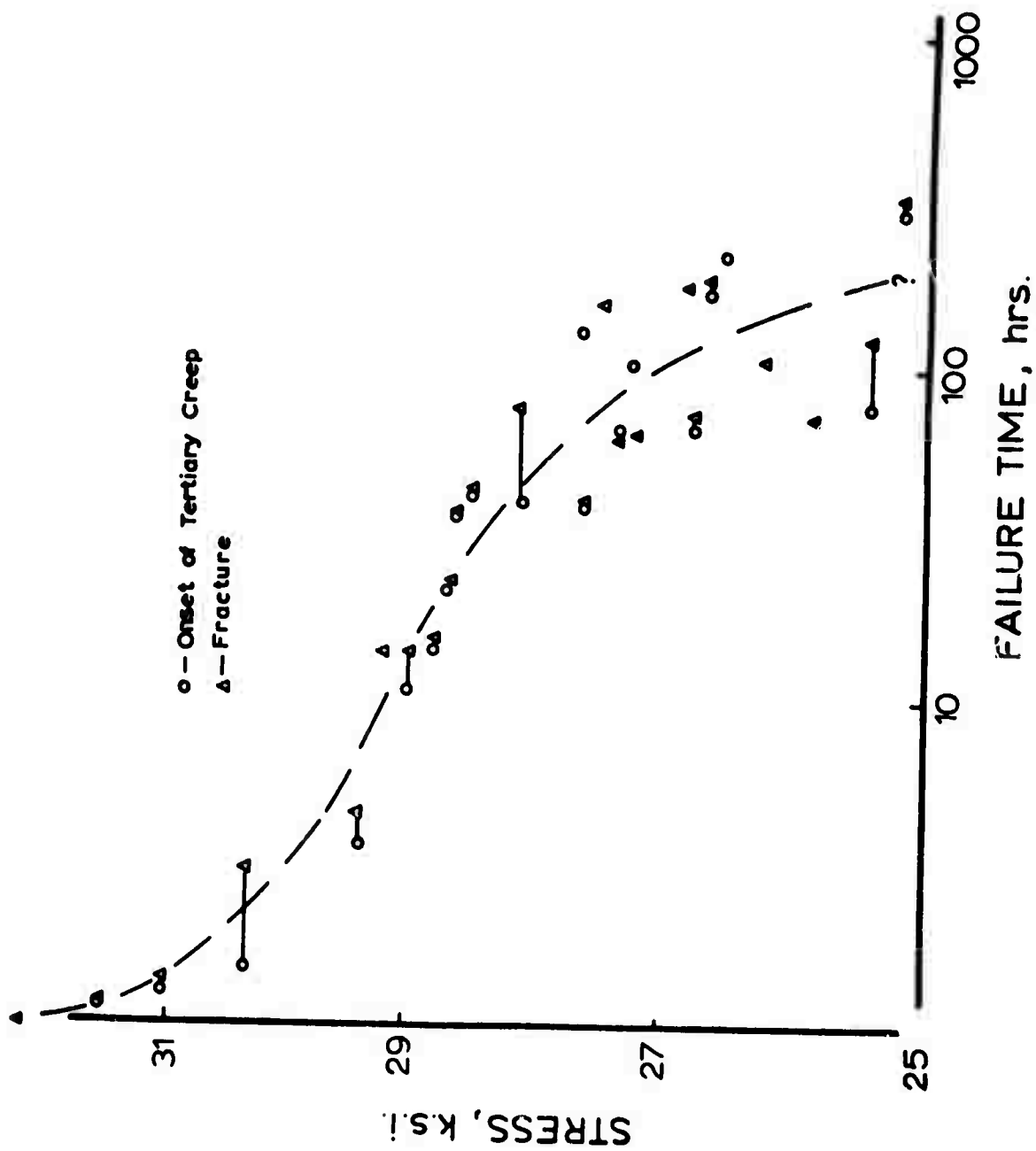
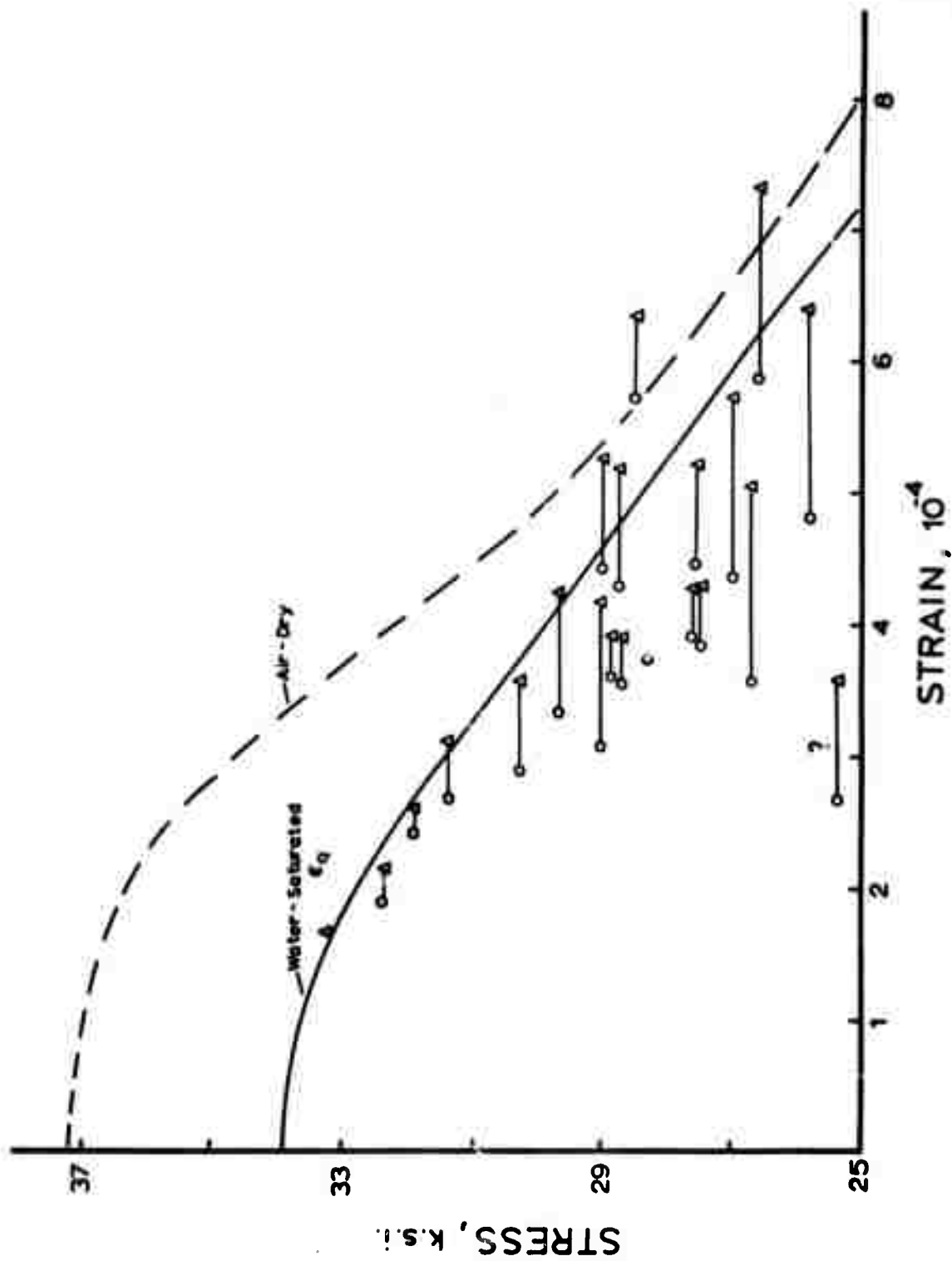FIGURE 21. Strength-time relationship for Westerly granite

FIGURE 22. Stress-failure strain data for Westerly granite (curve: strain between ascending and descending parts of complete stress-strain curve; circles: onset of tertiary creep; triangles: creep fracture)
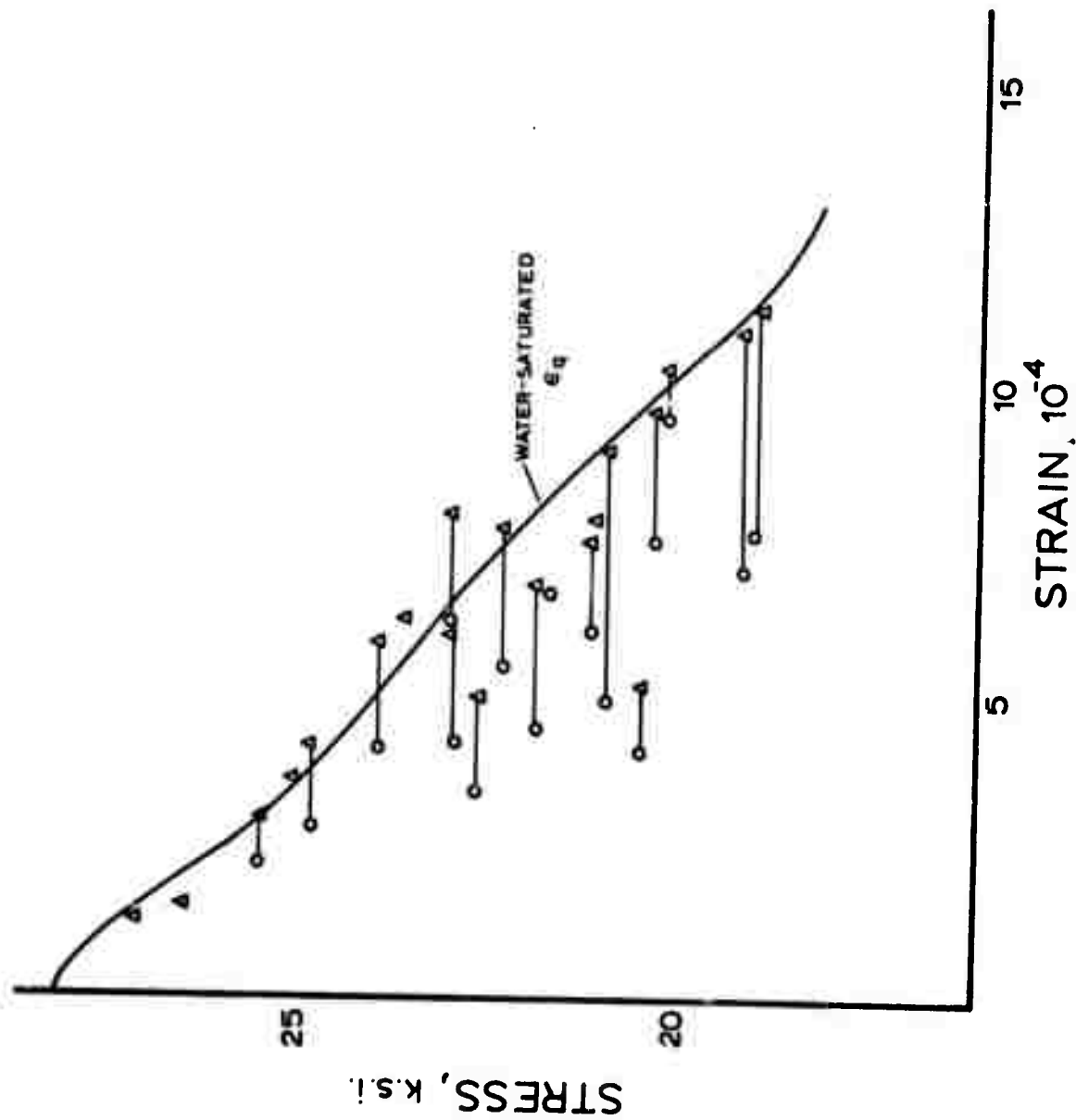
FIGURE 23. Stress-failure strain data for Nugget sandstone (curve: strain between ascending and descending parts of complete stress-strain curve; circles: onset of tertiary creep; triangles: creep fracture)

FIGURE 24. Stress-failure strain data for Tennessee marble (curve: strain between ascending and descending parts of complete stress-strain curve; circles: onset of tertiary creep; triangles: creep fracture)
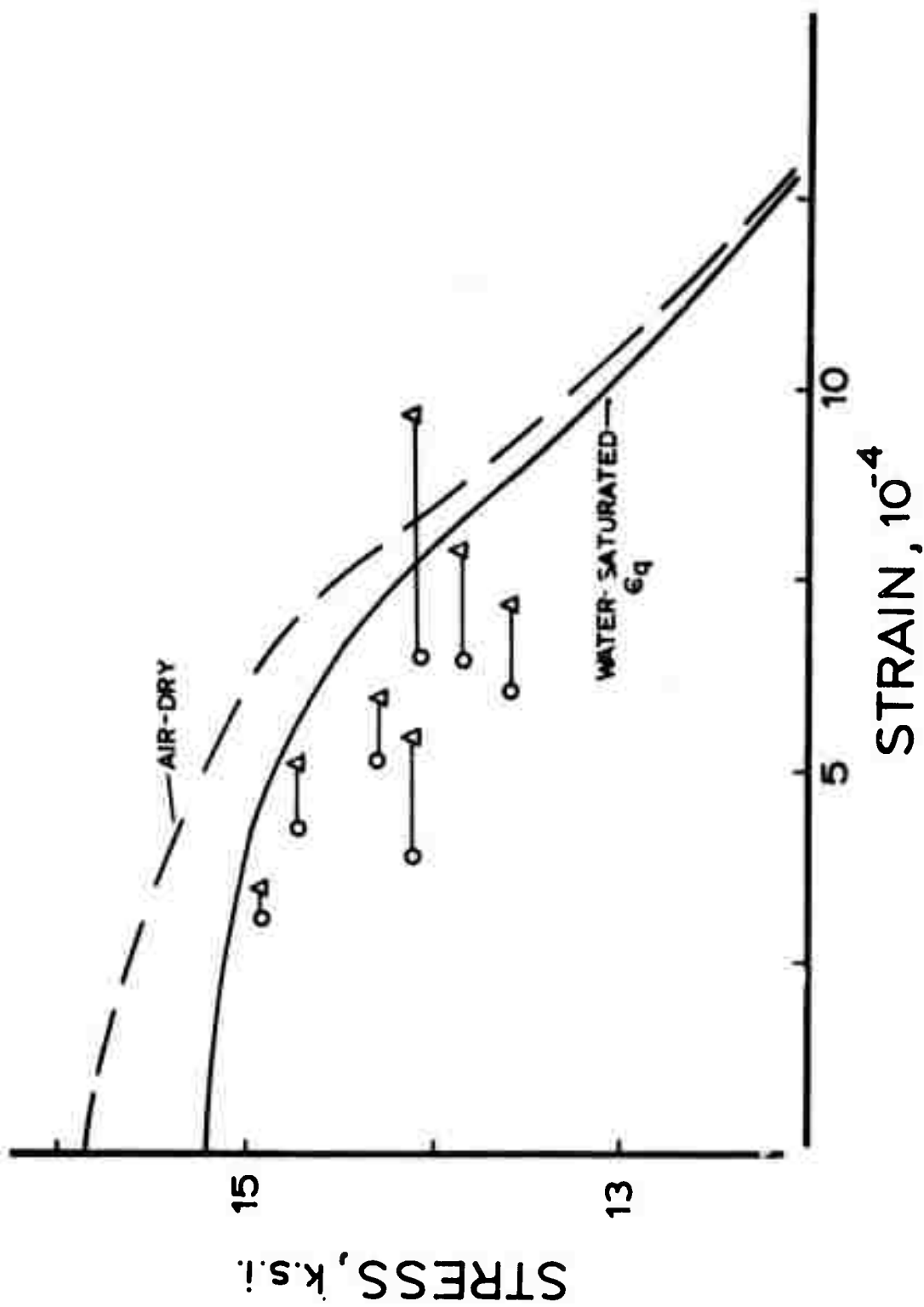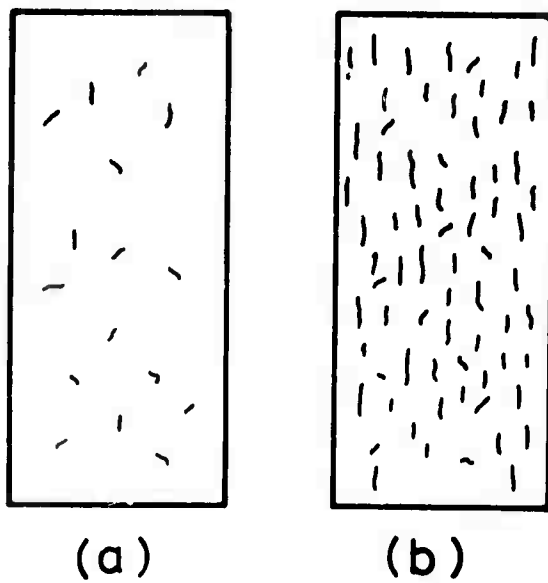
FIGURE 25. Diagrammatic representation of failure
patterns in Tennessee marble

FIGURE 26. Creep induced failure patterns in Nugget sandstone, sample no. 34 subjected to 19,000 psi for 1,475 hours

APPENDIX

DERIVATION OF STRESS STRAIN LAWS FOR GRANITE AND SANDSTONE SUBJECTED TO UNIAXIAL COMPRESSION

Time dependent stress-strain laws for granite and sandstone were derived from a description of primary and secondary creep.

Westerly Granite

Primary Creep

Primary creep in water saturated Westerly granite was defined by an equation of the from:

$$\log \varepsilon_I = n\log t + C \qquad (A1)$$

or $\qquad \varepsilon_I = 10^C t^n$

If a constant stress is applied at time zero and if the time t is expressed in hours then C denotes the strain accumulation which takes place during the first hour of creep. By and large, the magnitude of C is a function of the prevailing stress level. m is independent of the applied uniaxial compressive stress. To ascertain m and C, all primary creep data were plotted in $\log\varepsilon$, log t space. Then n was calculated as the mean slope:

$$n = 0.392$$

The stress dependency of C was evaluated from plots C versus stress, σ, as shown in Figure 16. The large scatter of data in Figure 1 created some difficulties in the assessment of C. It appears that C is constant up to a "threshold" stress $\sigma \approx 27{,}000$ psi. For $\sigma \geq 27{,}000$ psi, C appears to vary linearly with stress, i.e.

$$\sigma = a C + b \qquad (A2)$$

To simplify the analysis, Equation A2 was assumed to hold for all $\sigma \geq \sigma^*$

where σ^* denotes half of the mean quasi-static compressive strength, σ_c, of air-dried Westerly granite. Hence:

$$\sigma^* = 18,750 \text{ psi}$$

σ^* may be interpreted as the threshold stress above which creep is controlled primarily by micro-cracking. The constants a and b in Equation A2 were calculated by means of Figure 16.

Accordingly,

$$a = 0.964 \times 10^4$$

and

$$b = 6.8 \times 10^4$$

Thus

$$\sigma = (0.964 \, C + 6.8) \, 10^4 \tag{A3}$$

Equation A3 is recast into a more convenient form by means of

$$\sigma^* = 18,750 = (0.964 C^* + 6.8) \, 10^4 \tag{A4}$$

Dividing equation A3 by equation A4, in general,

$$\frac{\sigma}{\sigma^*} = \frac{aC + b}{aC^* + b} \tag{A5}$$

Solving for C renders,

$$C = \frac{\sigma}{\sigma^*} \left(C^* + \frac{b}{a} \right) - \frac{b}{a} \tag{A6}$$

Substituting for a and b and using equation A4:

$$C = 1.95 \frac{\sigma}{\sigma^*} - 7.06$$

Therefore

$$\varepsilon_I = 10^C \, t^n = 8.7 \times 10^{-8} \times 10^{1.95 \frac{\sigma}{\sigma}} \, t^{0.392}$$

or

$$\varepsilon_I = Be^{N\frac{\sigma}{\sigma^*}} \, t^n \tag{A7}$$

where $B = 8.7 \times 10^{-8}$

$N = 4.49$

$n = 0.392$

$\sigma^* = 18,750 \text{ psi}$

$\frac{\sigma}{\sigma^*} \leq 2$

Equation A7 defined primary creep as a function of current stress and time. However, the results of differential creep experiments indicate that primary creep is better described in terms of current stress and strain. This observation strongly suggests a strain hardening model. To derive an equation which accounts for strain hardening care must be exercised in the definition of stress. If the stress is held constant then differentiation of Equation A7 yields:

$$\dot{\epsilon}_I = \frac{d\epsilon_I}{dt} = n B e^{n\frac{\sigma}{\sigma^*}} t^{n-1} \tag{A8}$$

If equation A7 is used to eliminate the time t in equation A8

$$\dot{\epsilon}_I = \bar{B} e^{\bar{N}\frac{\sigma}{\sigma^*}} \epsilon_I^{1-\frac{1}{n}} \tag{A9}$$

where

$$\bar{B} = n B^{\frac{1}{n}} = 1.33 \times 10^{-20}$$

$$\bar{N} = \frac{N}{n} = 11.44$$

In turn, if the stress varies with time then

$$\dot{\epsilon}_I = (B \frac{N}{\sigma^*} e^{N\frac{\sigma^*}{\sigma}} \dot{\sigma}) t^n + nBe^{N\frac{\sigma}{\sigma^*}} t^{n-1} \tag{A10}$$

Therefore, expressing t in terms of the strain ϵ_I,

$$\dot{\epsilon}_I = \bar{\bar{B}} \epsilon_I \dot{\sigma} + \bar{B} e^{\bar{N}\frac{\sigma}{\sigma^*}} \epsilon_I^{1-\frac{1}{n}} \tag{A11}$$

where

$$\bar{\bar{B}} = 2.08 \times 10^{-11}$$

Equation A11 complicates matters considerably. Fortunately, a quick numerical check shows that the first term on the right hand side of Equation A11 becomes significant only if the strain rate corresponding to $\dot{\sigma}$ is equal or greater than 10^{-1} sec^{-1}. Hence, calculations of long-term time dependent strains can be made with the aid of the simpler

strain hardening equation A9.

Secondary Creep

During secondary creep, the creep rate varies linearly with time under constant environmental conditions. As a result, the analysis of the secondary creep data presented here is simple. Figure 17 shows that:

$$\log \dot{\varepsilon}_{II} = m\sigma + d \tag{A12}$$

using a least square fit

$$m = 5 \times 10^{-4}$$

and

$$d = -22.68$$

Equation A12 is again recast by introducing the "threshold" stress $\sigma^* = 18,750$ psi Since

$$\log \dot{\varepsilon}^* = m\sigma^* - d$$

and

$$\log \frac{\dot{\varepsilon}_{II}}{\dot{\varepsilon}^*} = m(\sigma - \sigma^*)$$

$$\dot{\varepsilon}_{II} = \dot{\varepsilon}^* \, 10^{-m\sigma^*} \, 10^{\,m\sigma^*} \left(\frac{\sigma}{\sigma^*}\right)$$

$$\varepsilon_{II} = De^{\overline{M}\frac{\sigma}{\sigma^*}} \tag{A13}$$

where

$$D = 7.17 \times 10^{-20}$$
$$\overline{M} = 21.6$$
$$\sigma^* = 18,750 \text{ psi}$$

$$\frac{\sigma}{\sigma^*} \le 2$$

Total Time Dependent Strain

To a first approximation, the total creep in Westerly granite is obtained by adding Equations A9 and A13:

$$\dot{\varepsilon} = \dot{\varepsilon}_I + \dot{\varepsilon}_{II} = \overline{B}e^{\overline{N}\frac{\sigma}{\sigma^*}} \varepsilon_I^{1-\frac{1}{n}} + D_2 e^{\overline{M}\frac{\sigma}{\sigma^*}}$$

Renaming all coefficients:

$$\dot{\varepsilon} = A \varepsilon^{a_1} e^{a_2\frac{\sigma}{\sigma^*}} + A_2 e^{a_3\frac{\sigma}{\sigma^*}} \tag{A14}$$

where

$$A_1 = \overline{B} = 1.33 \times 10^{-20}$$

$$A_2 = D = 7.17 \times 10^{-20}$$

$$a_1 = 1 - \frac{1}{n}; \quad n = 0.392$$

$$a_2 = \overline{N} = 11.44$$

$$a_3 = \overline{M} = 21.6$$

$$\sigma^* = 18,750 \text{ psi}$$

Equations A 9 and A13 and A14 are not restricted to conditions of constant stress. However, to what extent they are valid under general loading conditions requires further experiments to be conducted. Obviously, they do not include the influence of temperature and pore water pressure.

Nugget Sandstone

Primary Creep

The data for water saturated Nugget sandstone were analyzed in the same manner as the data for Westerly granite. All primary creep data were fit to the expression:

$$\log \varepsilon_I = n \log t + C \tag{A1}$$

or

$$\varepsilon_I = 10^C t^n$$

Again n is the mean slope of double logarithmic plots of strain versus time.

Accordingly: $\qquad n = 0.29$

m is assumed to be stress independent.

To express C as a function of stress, Figure 18 was employed. Thus:

$$\sigma = a\,C + b$$

where $\qquad a = 0.667 \times 10^4$

$\qquad\qquad b = 4.46 \times 10^4$

Introducing a "threshold" stress σ^* equal to half the quasi-static uniaxial compressive strength of air-dried Nugget sandstone.

$$\sigma^* = 16,700 \text{ psi}$$

Equation A1 becomes:

$$\varepsilon_I = 10_c\, t_n = 10^{-7}\, e^{5.75\frac{\sigma}{\sigma^*}}\, t^{0.29}$$

or $\qquad \varepsilon_I = Be^{N\frac{\sigma}{\sigma^*}}\, t^n \qquad\qquad\qquad\qquad$ (A7)

where $\qquad B = 10^{-7}$

$\qquad\qquad N = 5.75$

$\qquad\qquad n = 0.29$

$\qquad\qquad \sigma^* = 18,750$

$\qquad\qquad \dfrac{\sigma}{\sigma^*} \le 2$

Using the strain hardening model Equation A9 finally:

$$\dot{\varepsilon}_I = \bar{B}\, e^{\bar{N}\frac{\sigma}{\sigma^*}}\, \varepsilon^{1-\frac{1}{n}}$$

where $\qquad \bar{B} = nB^{\frac{1}{n}} = 2.11 \times 10^{-25}$

$\qquad\qquad \bar{N} = \dfrac{N}{n} = 19.83$

$\qquad\qquad n = 0.29$

Secondary Creep

From Figure 19:

$$\log \dot{\varepsilon}_{II} = m\,\sigma + d$$

A least square fit to the data shown in Figure rendered:

$$m = 0.706 \times 10^{-4}$$

$$d = -23.43$$

With $\sigma^* = 16{,}700$ psi

$$\dot{\varepsilon}_{II} = 1.339 \times 10^{-20}\, e^{\,27.2\frac{\sigma}{\sigma^*}}$$

or

$$\dot{\varepsilon}_{II} = D\, e^{\overline{M}\frac{\sigma}{\sigma^*}} \tag{A13}$$

where

$$D = 1.339 \times 10^{-20}$$

$$\overline{M} = 27.2$$

$$\sigma^* = 16.700 \text{ psi}$$

$$\frac{\sigma}{\sigma^*} \leq 2$$

Total Strain

$$\dot{\varepsilon} = \dot{\varepsilon}_I + \dot{\varepsilon}_{II} = A_1 \varepsilon^{a_1} e^{a_2\frac{\sigma}{\sigma^*}} + A_2 e^{a_3\frac{\sigma}{\sigma^*}}$$

$$A_1 = \overline{B} = 2.11 \times 10^{-25}$$

$$A_2 = D = 1.339 \times 10^{-20}$$

$$a_1 = 1 - \frac{1}{n}\; ;\; n = 0.29$$

$$a_2 = \overline{N} = 19.83$$

$$a_3 = \overline{M} = 27.2$$

$$\sigma^* = 16{,}700 \text{ psi}$$